TYPE 1 DIABETES

Human hypoimmune primary pancreatic islets avoid rejection and autoimmunity and alleviate diabetes in allogeneic humanized mice

Xiaomeng Hu[1], Corie Gattis[1], Ari G. Olroyd[1], Annabelle M. Friera[1], Kathy White[1], Chi Young[1], Ron Basco[1], Meghan Lamba[1], Frank Wells[1], Ramya Ankala[1], William E. Dowdle[1], August Lin[1], Kyla Egenberger[1], J. Michael Rukstalis[1], Jeffrey R. Millman[1], Andrew J. Connolly[2], Tobias Deuse[3]†, Sonja Schrepfer[1]*†

Transplantation of allogeneic pancreatic donor islets has successfully been performed in selected patients with difficult-to-control insulin-dependent diabetes and impaired awareness of hypoglycemia (IAH). However, the required systemic immunosuppression associated with this procedure prevents this cell replacement therapy from more widespread adoption in larger patient populations. We report the editing of primary human islet cells to the hypoimmune HLA class I– and class II–negative and CD47-overexpressing phenotype and their re-aggregation into human HIP pseudoislets (p-islets). Human HIP p-islets were shown to survive, engraft, and ameliorate diabetes in immunocompetent, allogeneic, diabetic humanized mice. HIP p-islet cells were further shown to avoid autoimmune killing in autologous, diabetic humanized autoimmune mice. The survival and endocrine function of HIP p-islet cells were not impaired by contamination of unedited or partially edited cells within the p-islets. HIP p-islet cells were eliminated quickly and reliably in this model using a CD47-targeting antibody, thus providing a safety strategy in case HIP cells exert toxicity in a future clinical setting. Transplantation of human HIP p-islets for which no immunosuppression is required has the potential to lead to wider adoption of this therapy and help more diabetes patients with IAH and history of severe hypoglycemic events to achieve insulin independence.

INTRODUCTION

Insulin has been used to treat patients with type 1 diabetes mellitus (T1DM) for 100 years and has transformed the once-fatal diagnosis into a chronic, medically manageable condition (*1*). However, morbidity, mortality, and quality of life remain a problem (*2*, *3*), specifically for 25% of patients with impaired awareness of hypoglycemia (IAH) who are at high risk of severe hypoglycemic events and associated morbidities (*4*, *5*). In addition, half of all patients with long-standing T1DM require assistance for severe hypoglycemic events, which increases their risk to that of patients with IAH (*6*). The risk for severe hypoglycemic events increases with the duration of T1DM (*7*). Continuous glucose monitoring has shown the ability to catch peaks or drops in glucose concentrations better than conventional fingerstick blood glucose meter checks and has improved glycemic control in adults (*8*, *9*) as well as adolescents and young adults with T1DM (*10*). Such wearable bioartificial devices provide glucose readings, trends, and alerts to the user in real time to inform diabetes treatment decisions (*11*), but compared with the physiological, immediate β cell response, integrated closed-loop systems still face delays in subcutaneous glucose sensing and insulin delivery, and patients experience an average of at least 30 min each day with glucose less than 3.9 mM (*12*). These systems are appreciated by most patients but do not provide curative therapy of T1DM or completely remove the burden of glucose uncertainty and unremitting daily self-management. The key negative themes include technical difficulties, intrusiveness of alarms, and equipment size (*13*).

Allogeneic islet transplantation replenishes the vanished β cell population (*14*), and clinical trials in patients with IAH and history of severe hypoglycemic events showed that it provides glycemic control, restoration of hypoglycemia awareness, and protection from severe hypoglycemic events (*15*, *16*). Twenty-year follow-up data of allogeneic islet transplantation reported a mean duration of islet graft function of 4.4 to 5.9 years on immunosuppression (*17*, *18*). However, critical challenges to allogeneic islet transplantation include an unsolved regulatory framework (*19*), early loss of transplanted islets from instant blood-mediated inflammatory reaction (*20*, *21*), and the need for life-long immunosuppression to protect the islet grafts from allo- and autoimmunity. Immunosuppression causes most side effects, including β cell toxicity (*22*), kidney toxicity (*23*, *24*), infections (*25*), and cancer (*26*), and limits the more widespread use of this strategy. We here report the concept of human allogeneic, gene-engineered hypoimmune (HIP) islets for transplantation without the need for immunosuppression. Allogeneic HIP islets circumvent allogeneic and autoimmune responses and provide glycemic control in preclinical models.

RESULTS

Engineering of HIP-edited primary human pseudoislets

Primary human islets isolated from organ donors are sensitive to hypoxia and stress and had already undergone the isolation

[1]Sana Biotechnology Inc., 1 Tower Place, South San Francisco, CA 94080, USA. [2]Department of Pathology, University of California, San Francisco, San Francisco, CA 94143, USA. [3]Department of Surgery, Division of Cardiothoracic Surgery, Transplant and Stem Cell Immunobiology (TSI) Lab, University of California, San Francisco, San Francisco, CA 94143, USA.
*Corresponding author. Email: sonja.schrepfer@sana.com
†These authors contributed equally to this work.

process, culturing, and shipping to our facility before we could start the editing process. We adopted the strategy to dissociate islets into single cells for each step of engineering or cell sorting and immediately allowed the cells to reaggregate thereafter into pseudoislets (p-islets). Primary human islets were dissociated for the inactivation of the *B2M* and *CIITA* genes using CRISPR guide RNAs (gRNAs) and Cas9. Cells negative for human leukocyte antigen (HLA) class I and class II expression in flow cytometry were then sorted, and these islet cells were transduced with lentiviral particles carrying transgenes for CD47 and firefly luciferase. Cells overexpressing CD47 (measured by flow cytometry) were subsequently sorted to generate hypoimmune HLA class I– and class II–deficient CD47-overexpressing (HIP) p-islets (fig. S1A). Wild-type (WT) p-islets were generated in parallel, and the cells underwent the same dissociation and reaggregation steps without the engineering and sorting. The HIP phenotype was stable and was not affected by interferon-γ (IFN-γ) and tumor necrosis factor–α stimulation (fig. S1B). The generated WT and HIP p-islets showed similar size, cell type composition, and in vitro insulin secretion, showing that the editing itself did not affect the morphology or endocrine function of the organoids (Fig. 1, A and B). HIP and WT p-islets demonstrated the expected immune phenotype (Fig. 1, A and C). Next, we aimed to assess the survival of p-islets and their cell composition in immunocompetent, diabetic allogeneic humanized NSG-SGM3 mice (*27*). The triple transgenic NSG-SGM3 mice were engineered from NSG mice and express human interleukin-3 (IL-3), granulocyte-macrophage colony-stimulating factor (GM-CSF), and stem cell factor, which provide cytokine support for the improved engraftment of human immune cells. A total of 300 WT or HIP p-islet clusters were injected into the hindlimb muscle and were recovered on the same day or 7 or 28 days later (Fig. 1D). WT p-islets could only be recovered on the same day but were fully rejected and dissolved at later time points (Fig. 1, E and F). In contrast, the total cell count and cell composition of HIP islets did not change over time (Fig. 1, G and H).

Human HIP p-islets are resilient and effective endocrine organoids

The survival, engraftment, and the ability to control diabetes were assessed in immunodeficient NSG mice to avoid immune rejection. Diabetes was induced using streptozotocin (STZ), and all mice had fasting glucose concentrations >400 mg/dl on the day of p-islet graft transplantation. Three hundred human WT or HIP p-islets were intramuscularly injected, and their survival was monitored by bioluminescence imaging (BLI). Both WT (fig. S2, A to D) and HIP p-islets (fig. S2, E to H) showed cell survival and similarly robust engraftment with improvement of their metabolic activity over time. WT and HIP p-islets achieved glycemic control within about 2 weeks and generated similar c-peptide concentrations 1 month after transplantation. These functional data confirmed that HIP-

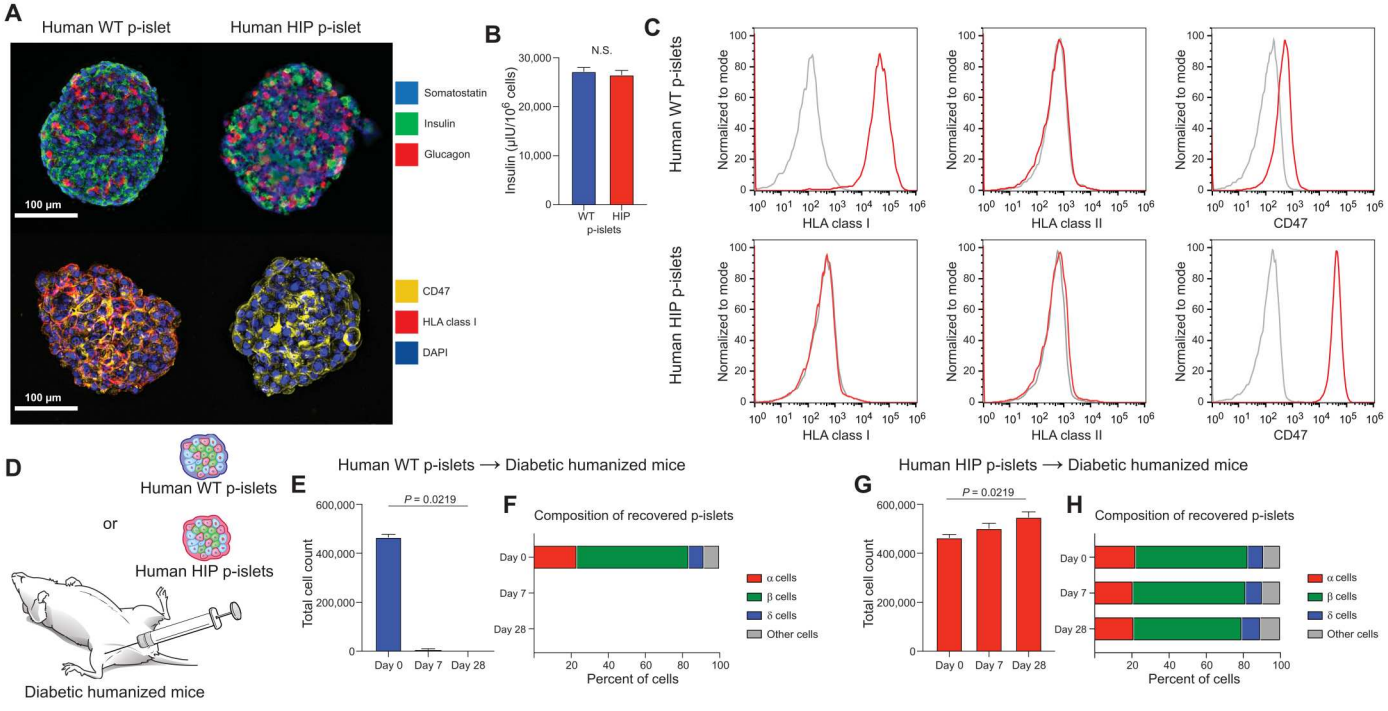

Fig. 1. Stable WT and HIP p-islets are engineered from primary human donor islets. (**A**) In vitro immunofluorescence stainings of human WT and HIP p-islets for somatostatin, insulin, and glucagon (representative pictures of two independent experiments). Additional immunofluorescence stainings for CD47, HLA class I, and DAPI (representative pictures of two independent experiments). (**B**) Insulin release of in vitro human WT and HIP p-islets was assessed by ELISA (means ± SD, three independent replicates per group, two-tailed Student's *t* test). (**C**) HLA class I and II and CD47 expression was assessed by flow cytometry (representative histograms of two independent experiments). (**D**) A total of 300 green fluorescent protein (GFP)–expressing human WT or HIP islets were transplanted into the hindlimb muscles of immunocompetent, diabetic allogeneic humanized NSG-SGM3 mice (three mice per group). (**E** to **H**) In each group, the hindlimb muscle was recovered after 0, 7, and 28 days in $n = 3$ animals, and transplanted islet cells were recovered. The total amount of GFP^+ cells was assessed by flow cytometry [(E and G), $n = 3$ mice per time point, Kruskal-Wallis test with Dunn's multiple comparisons test]. The composition of cell types was assessed by flow cytometry [(F and H), mean of $n = 3$ mice per time point].

edited p-islet cells maintained their endocrine function and showed unimpaired resilience toward the transplantation procedure.

The HIP p-islet cells' pharmacodynamics were studied by transplanting different amounts of p-islet clusters. In addition to the above study with 300 clusters, NSG groups with only 50, 100, or 150 clusters were used (fig. S2, I to R). All HIP p-islets survived without any dose-dependent differences. However, we observed a delay in glycemic control when injecting fewer transplanted p-islet clusters, although all mice eventually achieved euglycemia with similar c-peptide concentrations and physiologic responses to glucose challenge. Overall, these data emphasize the effective endocrine function of human HIP p-islets, which have greater glucose-sensitive insulin secretion as compared with reported human induced pluripotent stem cells (iPSC)–derived islet-like organoids (*28*). Three hundred p-islets were used for all subsequent studies to allow for swift diabetic control in the HIP groups.

Human HIP p-islets survive, engraft, and ameliorate diabetes in immunocompetent, allogeneic, diabetic humanized mice

Islet grafts will have to overcome both alloimmunity and autoimmunity. Allorejection was assessed first using immunocompetent humanized recipients that were exposed to p-islet grafts. All allogeneic WT p-islet grafts were fully rejected over 7 to 10 days and showed no effect on blood glucose, not even temporarily, and animals had no detectable c-peptide after 1 month (Fig. 2, A to C). As shown previously, humanized allogeneic NSG-SGM3 mice consistently reject allogeneic cell transplants (*29*). In contrast, all HIP p-islet allografts survived (Fig. 2, D and E) and showed BLI signals similar to those in immunocompromised NSG mice. Glycemic control was achieved in all recipients of HIP p-islets, and the kinetics of glucose control were again similar to those in immunocompromised NSG mice (Fig. 2F), suggesting that the allogeneic immune system had no impact on HIP p-islet efficacy. To assess the effect of CD47 overexpression on the survival of HIP p-islets in allogeneic, diabetic humanized mice, human HLA-I/II double-knockout (DKO) p-islets were used as controls (Fig. 2G). DKO islet cells were deficient in HLA class I and II but did not have CD47 overexpression. All DKO p-islets were rejected in a similar time frame as the WT p-islets and similarly had no impact on blood glucose or c-peptide (Fig. 2, H and I). Together, these data confirmed the sufficient reconstitution of the immune system in these humanized mice, which can effectively reject WT grafts via adaptive cytotoxicity and DKO grafts via innate cytotoxicity. The hindlimb muscles of all animals were recovered after 1 month. No traces of WT p-islet grafts were found in any animals. In contrast, HIP p-islets showed the same morphology as before transplantation and contained α, β, and δ cells (Fig. 2, J to M). There was no immune cell infiltrate in or around the HIP p-islet cells (Fig. 2N and fig. S3). For immune assays, splenocytes and serum were also recovered from all animals 6 days after cell transplantation and showed markedly elevated IFN-γ spot frequencies and immunoglobulin M (IgM) donor-specific antibodies against the grafts in the WT group, supporting the notion of a strong adaptive alloresponse (Fig. 2, O and P). No adaptive immune response was seen in humanized mice that received DKO or HIP p-islets. Assays for innate immune responses showed natural killer (NK) cell and macrophage cytotoxicity only against DKO p-islets, not WT or HIP p-islets (Fig. 2, Q and R). Confirmatory killing assays showed T cell and complement-dependent antibody killing of WT p-islets and NK cells, macrophage killing of DKO p-islets, and no killing of HIP p-islets (Fig. 2S). Overall, these results support the sufficiency of our three-edit HIP concept to avoid all allogeneic immune cell attacks.

Murine HIP p-islets escape autoimmunity and alloimmunity in nonobese diabetic mice

To assess autoimmune killing, we initially switched to the murine system. Autoimmune diabetes has extensively been studied using nonobese diabetic (NOD) mice (*30*), which develop spontaneous T1DM with induction of autoantibodies (*31*) and autoreactive T cells (*32*). For our study, all NOD mice had established T1DM at the time that they were included in study groups. The engineering of pancreatic islets was done accordingly; *B2m* and *Ciita* were inactivated, and mouse CD47 was overexpressed. We found that the autoimmune response of NOD mice was directed specifically against islet cells because transplanted syngeneic NOD p-islets were rejected within about 2 weeks and had no impact on blood glucose concentrations (Fig. 3, A to C), whereas transplanted syngeneic NOD fibroblasts survived (Fig. 3, D and E). HIP-engineered syngeneic NOD p-islets (HIP NOD p-islets) effectively circumvented autoimmunity and survived in NOD mice and achieved glycemic control in less than 2 weeks (Fig. 3, F to H). Next, primary NOD islets were transplanted into NOD mice, and splenocytes and serum were recovered after 5 days. NOD splenocytes and serum expeditiously killed syngeneic NOD p-islets but spared HIP NOD p-islets in vitro, confirming the ability of HIP NOD p-islets to avoid NOD autoimmunity (Fig. 3, I and J). To test whether the NOD autoimmunity was strong enough to kill already engrafted p-islets, NOD or NOD HIP p-islets were transplanted into diabetic NSG mice with adoptive transfer of NOD splenocytes on day 11. NOD splenocytes quickly rejected already engrafted syngeneic NOD p-islets and reestablished diabetic blood glucose concentrations (Fig. 3, K to M). In contrast, NOD splenocytes did not affect the survival or endocrine activity of HIP NOD p-islets (Fig. 3, N to P). Next, we assessed whether NOD mice could reject allogeneic grafts and thereby serve as a model for both autoimmunity and alloimmunity. Allogeneic mouse C57BL/6 iPSC–derived endothelial cell (miEC) grafts were rejected in NOD mice, and splenocytes and serum recovered after 5 days killed C57BL/6 miECs in vitro (fig. S4, A to C). C57BL/6 miEC grafts survived in immunodeficient NOD severe combined immunodeficient (SCID) mice (fig. S4, D and E). Allogeneic C57BL/6 p-islets transplanted into NOD mice were rejected quickly and had no effect on blood glucose (Fig. 4, A to C), whereas allogeneic C57BL/6 HIP p-islets survived and normalized blood glucose (Fig. 4, D to F). Splenocytes and serum recovered after 5 days killed allogeneic C57BL/6 p-islet cells but not C57BL/6 HIP p-islet cells in vitro (Fig. 4, G and H). We next assessed whether the autoimmune response against syngeneic islets from NOD mice would also target already engrafted p-islet allografts. NOD splenocytes adoptively transferred to NSG mice with engrafted allogeneic C57BL/6 p-islets, and decreasing glucose concentrations caused graft failure and quickly reestablished diabetic hyperglycemia (Fig. 4, I to K). In contrast, adoptively transferred NOD splenocytes did not attack allogeneic C57BL/6 HIP p-islets and did not impede establishment of glycemic control (Fig. 4, L to N). C57BL/6 p-islets (Fig. 4, O to Q) and C57BL/6 HIP p-islets (Fig. 4, R to T) transplanted into NOD SCID mice that could not

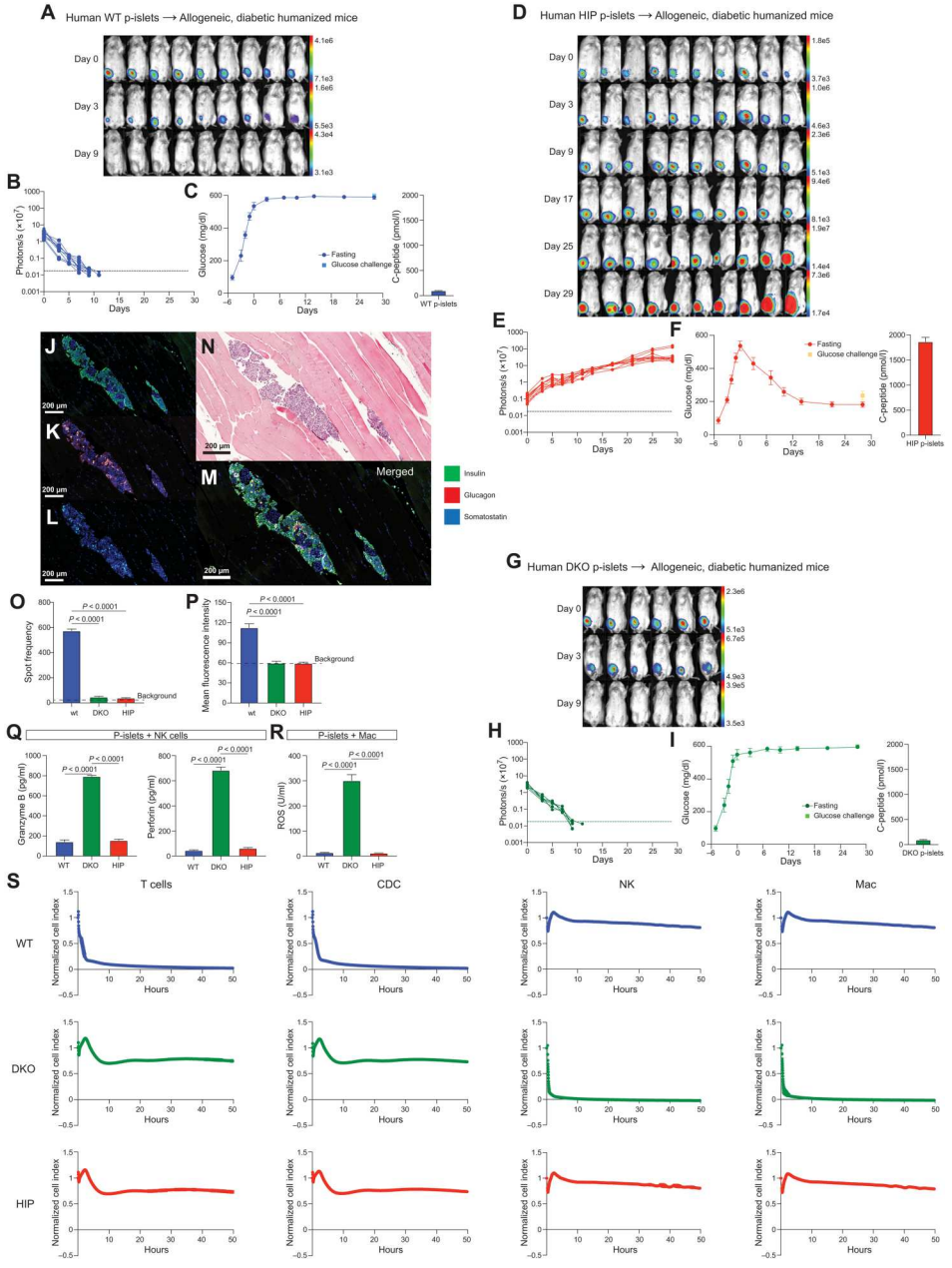

Fig. 2. Human HIP p-islets survive in immunocompetent, allogeneic, diabetic humanized mice and alleviate diabetes. (**A** and **B**) Human WT p-islets were transplanted into allogeneic, diabetic humanized mice. BLI (A) and signals (B) for all nine animals are shown. (**C**) Fasting blood glucose and 30-min glucose challenge are shown (means ± SD). Blood c-peptide was measured after 29 days (means ± SD, nine animals). (**D** and **E**) Human HIP p-islets were transplanted into allogeneic, diabetic humanized mice. BLI (D) and signals (E) for all 10 animals are shown. (**F**) Fasting blood glucose and 30-min glucose challenge are shown (means ± SD). Blood c-peptide was measured after 29 days (means ± SD, 10 animals). (**G** and **H**) Human DKO p-islets were transplanted into allogeneic, diabetic humanized mice. BLI (G) and signals (H) for all six animals are shown. (**I**) Fasting blood glucose and 30-min glucose challenge are shown (means ± SD). Blood c-peptide was measured after 29 days (means ± SD, six animals). (**J** to **M**) On day 29, hindlimb muscles were recovered and sectioned. Immunofluorescence staining [(J and L), merged in (M)] revealed morphologically normal HIP p-islets containing α, β, and δ cells. (**N**) Histology with hematoxylin and eosin staining showed the injected HIP p-islets without any adjacent immune cell infiltrates. (**O** and **P**) Human WT, DKO, or HIP p-islets were transplanted into additional allogeneic, diabetic humanized mice, and splenocytes and serum were recovered after 6 days. Enzyme-linked immunosorbent spot (ELISpot) assays with splenocytes against the transplanted islet cells were performed [(O), five animals per group, ANOVA with Bonferroni's post hoc test]. ELISpots with splenocytes from mice that received no transplants are shown as background. Donor-specific antibodies (DSAs) against the transplanted islet cells were assessed in flow cytometry [(P), five animals per group, ANOVA with Bonferroni's post hoc test]. Islet cells incubated with sera from mice that received no transplants are shown as background. (**Q**) Human WT, DKO, or HIP islet cells were incubated with allogeneic NK cells for 90 hours, and then granzyme B and perforin in the supernatant were quantified by ELISA (means ± SD, three independent replicates per group, ANOVA with Bonferroni's post hoc test). (**R**) Human WT, DKO, or HIP islet cells were incubated with allogeneic macrophages for 90 hours, and then ROS in the supernatant was quantified by ELISA (means ± SD, three independent replicates per group, ANOVA with Bonferroni's post hoc test). (**S**) In vitro impedance killing assays were performed with human WT, DKO, or HIP islet cells as targets and allogeneic T cells, serum [complement-dependent cytotoxicity (CDC)], NK cells, or macrophages (Mac) as effector system (means ± SD, three independent replicates per group and time point).

mount an allo- or autoimmune response showed similar graft survival and glucose control. Together, the data generated in NOD mice show that allogeneic mouse HIP p-islets effectively escape both autoimmunity and alloimmunity.

Human iPSC–derived HIP p-islets escape autoimmunity in autologous, diabetic humanized mice

We next aimed to recapitulate the above murine data in an autologous, humanized autoimmune diabetes model for human HIP p-islets. Peripheral blood mononuclear cells (PBMCs) from a patient with long-standing T1DM and measurable GAD65, ZT8, and IA-2 antibodies were used to engraft NSG-SGM3 mice (T1DM mice; Fig. 5A). Because β cells are destroyed in patients with T1DM, we generated iPSCs from the same PBMC pool; one fraction underwent HIP engineering (*B2M* and *CIITA* inactivation and CD47 and Luc overexpression), whereas the other fraction was transduced to overexpress Luc only, without HIP engineering. Both autologous (auto) and HIP auto p-islets (HIP) were then differentiated into autologous islet cells for subsequent transplantation into T1DM mice (Fig. 5A). Auto and HIP iPSC–derived p-islets showed

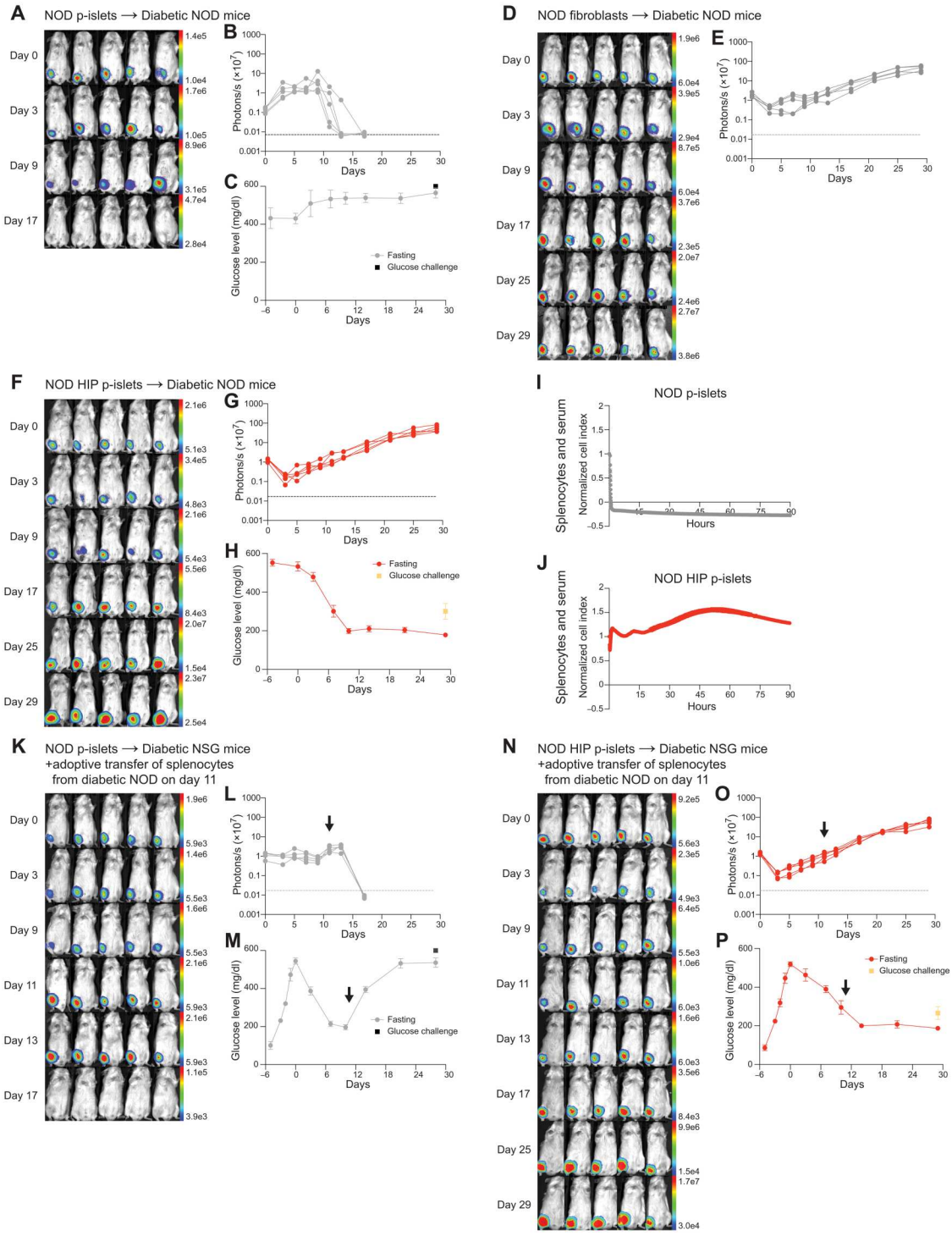

Fig. 3. Syngeneic murine HIP p-islets escape autoimmunity in NOD mice. (**A** and **B**) NOD p-islets were transplanted into syngeneic, NOD mice. BLI (A) and signals (B) for all five animals are shown. (**C**) Fasting blood glucose and 30-min glucose challenge are shown (means ± SD, five animals). (**D** and **E**) NOD fibroblasts were transplanted into syngeneic, NOD mice. BLI (D) and signals (E) for all five animals are shown. (**F** and **G**) NOD HIP p-islets were transplanted into syngeneic, NOD mice. BLI (F) and signals (G) for all five animals are shown. (**H**) Fasting blood glucose and 30-min glucose challenge are shown (means ± SD, five animals). (**I** and **J**) Primary NOD islets were transplanted into NOD mice, and splenocytes and serum were recovered after 5 days and used as effector system in impedance killing assays. NOD p-islet cells (I) or NOD HIP p-islet cells (J) were used as targets (means ± SD, five animals each). (**K** and **L**) NOD p-islets were transplanted into immunodeficient, diabetic NSG mice. BLI (K) and signals (L) for all five animals are shown. On day 11, splenocytes from NOD mice were adoptively transferred to these NSG mice. (**M**) Fasting blood glucose and 30-min glucose challenge are shown (means ± SD, five animals). (**N** and **O**) NOD HIP p-islets were transplanted into immunodeficient, diabetic NSG mice. BLI (N) and signals (O) for all five animals are shown. On day 11, splenocytes from NOD mice were adoptively transferred to these NSG mice. (**P**) Fasting blood glucose and 30-min glucose challenge are shown (means ± SD, five animals).

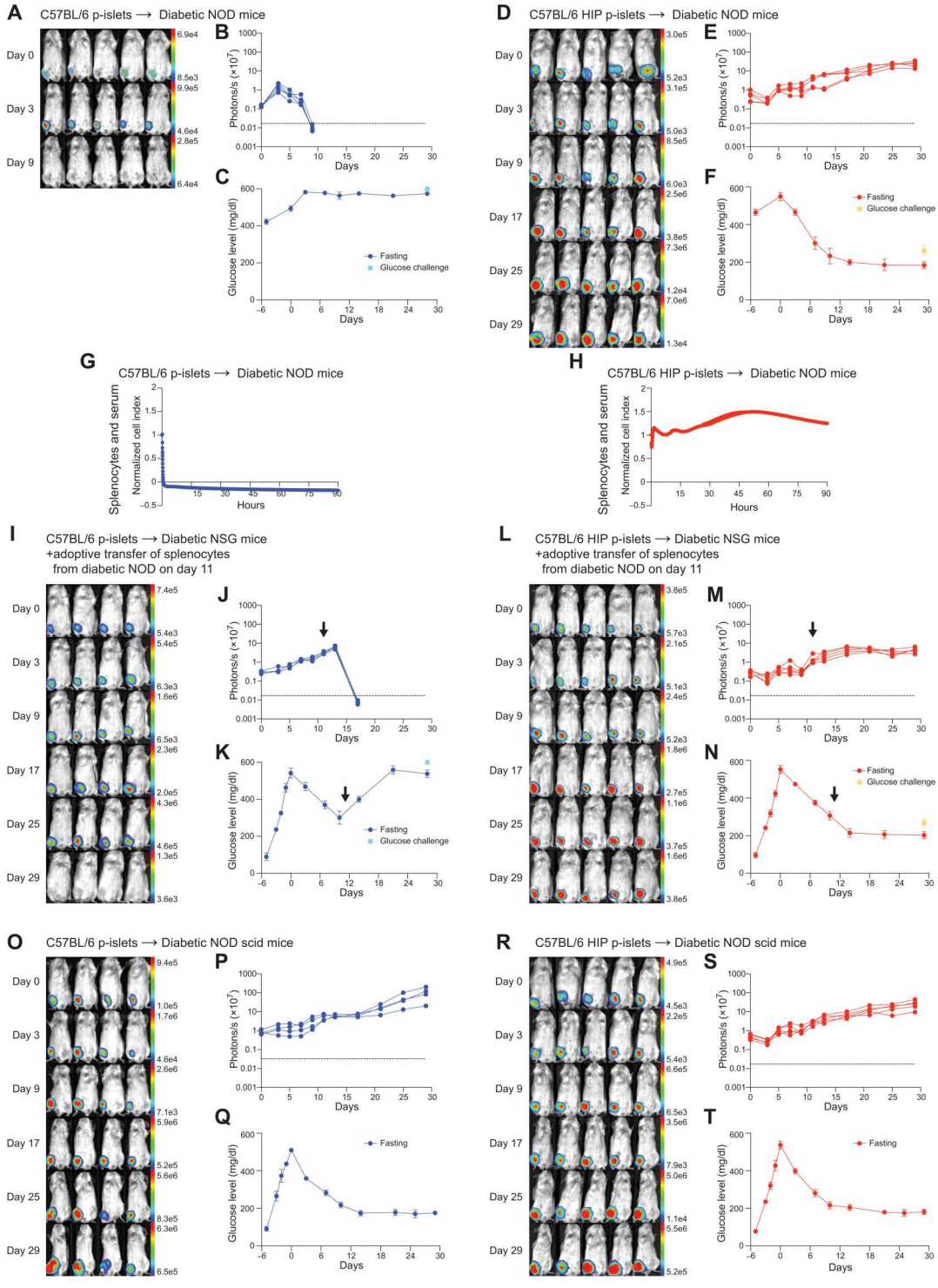

Fig. 4. Allogeneic murine HIP p-islets escape autoimmunity and alloimmunity in NOD mice. (**A** and **B**) Allogeneic C57BL/6 p-islets were transplanted into NOD mice. BLI (A) and signals (B) for all five animals are shown. (**C**) Fasting blood glucose and 30-min glucose challenge are shown (means ± SD, five animals). (**D** and **E**) Allogeneic C57BL/6 HIP p-islets were transplanted into NOD mice. BLI (D) and signals (E) for all five animals are shown. (**F**) Fasting blood glucose and 30-min glucose challenge are shown (means ± SD, five animals). (**G** and **H**) Splenocytes and serum were recovered from NOD mice that received C57BL/6 p-islets (G) or C57BL/6 HIP p-islets (H) 5 days after transplantation. Impedance killing assays were run against C57BL/6 p-islet cells (G) or C57BL/6 HIP p-islet cells (H) (mean ± SD, 5 animals). (**I** and **J**) C57BL/6 p-islets were transplanted into immunodeficient, diabetic NSG mice. BLI (I) and signals (J) for all five animals are shown. On day 11, splenocytes from NOD mice were adoptively transferred to these NSG mice. (**K**) Fasting blood glucose and 30-min glucose challenge are shown (means ± SD, five animals). (**L** and **M**) C57BL/6 HIP p-islets were transplanted into immunodeficient, diabetic NSG mice. BLI (L) and signals (M) for all five animals are shown. On day 11, splenocytes from NOD mice were adoptively transferred to these NSG mice. (**N**) Fasting blood glucose and 30-min glucose challenge are shown (means ± SD, five animals). (**O** and **P**) C57BL/6 p-islets were transplanted into immunodeficient, NOD SCID mice. BLI (O) and signals (P) for all five animals are shown. (**Q**) Fasting blood glucose is shown (means ± SD, five animals). (**R** and **S**) C57BL/6 HIP p-islets were transplanted into immunodeficient, NOD SCID mice. BLI (R) and signals (S) for all five animals are shown. (**T**) Fasting blood glucose is shown (means ± SD, five animals).

similar size, morphology, endocrine hormone content, and cell composition, but only HIP p-islets showed abundant CD47 and lack of HLA class I expression (Fig. 5, B to E). Both auto and HIP iPSC–derived p-islets released similar amounts of insulin in vitro (Fig. 5F). Auto and HIP iPSC–derived p-islets were then transplanted into the autologous T1DM mice. The first injection was made into the right thigh muscle, and a second injection of auto p-islets was made into recipients of HIP p-islets on day 15 (Fig. 6A). The experiment was performed three times. The auto p-islets vanished quickly over just 5 to 10 days, confirming the establishment of transferred human autoimmune disease in these T1DM mice (Fig. 6, B and C). Transplantation of auto p-islets had no effect on blood glucose (Fig. 6D). Impedance-based killing assays with splenocytes and sera from T1DM mice that rejected auto p-islets also killed auto

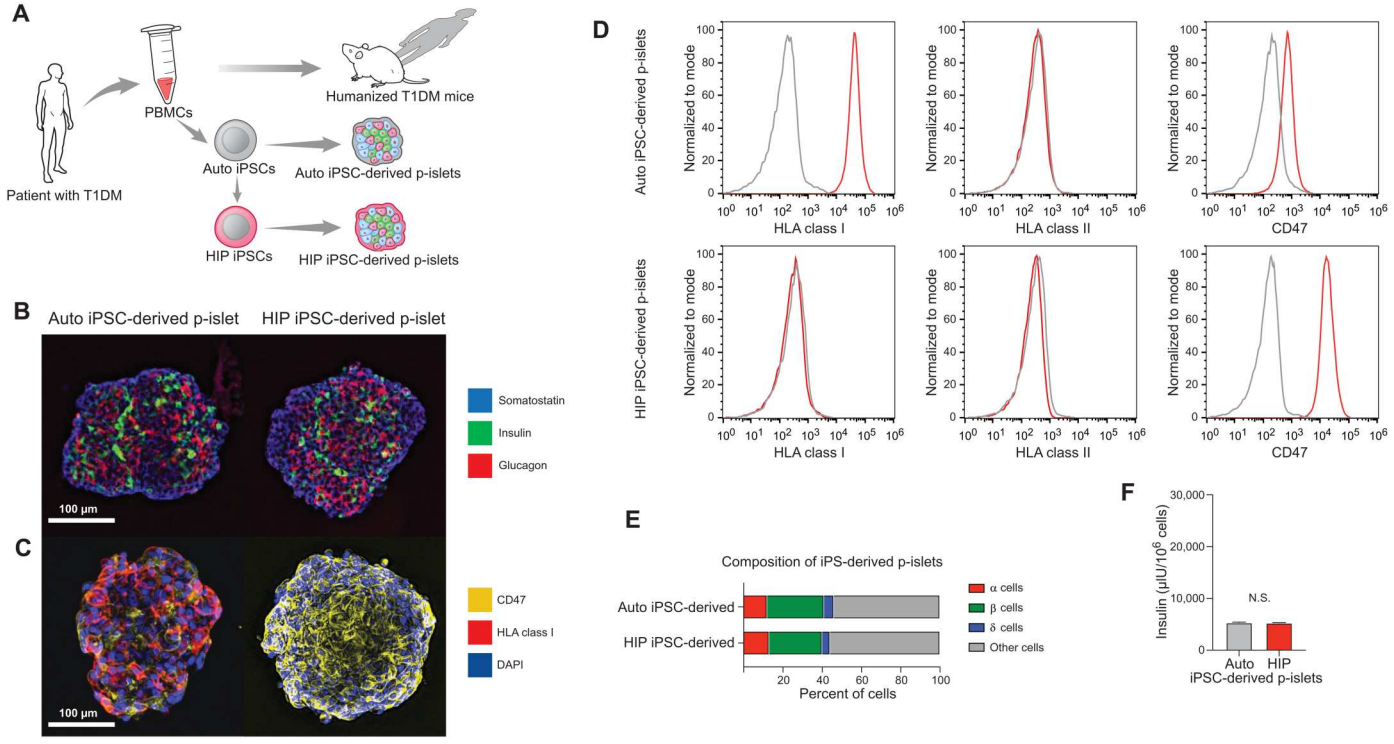

Fig. 5. A humanized mouse model for autoimmune diabetes. (**A**) PBMCs from a patient with T1DM were used to engraft NSG-SGM3 mice (T1DM mice) and to generate autologous (auto) p-islets through reprogramming to iPSCs and differentiation into islet cells. Some auto iPSCs underwent HIP editing, and these HIP iPSCs were differentiated into autologous HIP p-islets. (**B**) In vitro immunofluorescence staining of auto and HIP iPSC–derived p-islets for somatostatin, insulin, and glucagon (representative pictures of two independent experiments). (**C**) Additional immunofluorescence stainings for CD47, HLA class I, and DAPI (representative pictures of two independent experiments). (**D**) HLA class I and II and CD47 expression was assessed by flow cytometry (representative histograms of two independent experiments). (**E**) The composition of cell types in auto and HIP iPSC–derived p-islets was assessed by flow cytometry (mean of three experiments). (**F**) Insulin release of in vitro human auto and HIP iPSC–derived p-islets is assessed by ELISA (means ± SD, three independent replicates per group, two-tailed Student's *t* test).

p-islet cells in vitro (Fig. 6E). Auto p-islet cells were not killed by NK cells or macrophages (Fig. 6F). HIP iPSC–derived p-islets survived in T1DM mice, and their survival was not affected by the fact that subsequently transplanted auto p-islets were rejected in the same mice (Fig. 6, G and H). HIP iPSC–derived p-islets reliably achieved glycemic control in the animals within 2 weeks (Fig. 6I). In vitro killing assays with splenocytes and sera from T1DM mice that received HIP iPSC–derived p-islets and subsequently auto iPSC–derived p-islets confirmed that there was no immune response against HIP iPSC–derived p-islet cells (Fig. 6J). In addition, there was no NK cell or macrophage killing of HIP iPSC–derived p-islet cells (Fig. 6K). On day 29, only T1DM mice that received HIP iPSC–derived p-islets had relevant c-peptide concentrations (Fig. 6L). Together, these experiments showed that HIP iPSC–derived p-islets efficiently avoid autoimmune killing in a humanized model.

Human HIP p-islets are potentially well suited to overcome key immunological and pharmacologic stressors associated with clinical transplantation

Our stringent multistep protocol of gene engineering, flow cytometry sorting, and reaggregation into HIP p-islets would need to be modified to allow good manufacturing practice before human HIP p-islets can be tested in clinical trials. The efficiency of generating fully engineered cells will most likely be lower, and the clinical cell product could contain fractions of unengineered or DKO-edited cells. To test how contamination with WT or DKO cells within the HIP p-islets affects overall organoid survival and function, we performed experiments with 1:1 mixtures of cells. First, WT and HIP islet cells were reaggregated into p-islets and transplanted into allogeneic, diabetic humanized mice. BLI showed that the Luc^+ WT p-islet fraction vanished over 10 days (Fig. 7, A and B). Luc^+ HIP p-islet cells, on the other hand, successfully engrafted and survived for the duration of the experiment (Fig. 7, D and E). Glucose monitoring in both experiments showed normalization of blood glucose by the prevailing HIP p-islet fraction (Fig. 7, C and F). Similarly, mixed DKO and HIP islets were reaggregated and transplanted into allogeneic, diabetic humanized mice. When the DKO fraction was labeled with Luc^+, we observed rapid disappearance of Luc^+ cells (Fig. 7, G and H), whereas in the Luc^+ HIP mixtures, the signal persisted for the duration of the experiment (Fig. 7, J and K). Again, glucose monitoring showed that the DKO/HIP p-islet mixtures were also effective at restoring glycemic control in these mice (Fig. 7, I and L). Together, these results demonstrate that as long as there are enough HIP p-islet cells, contamination with unengineered or partially engineered cells does not jeopardize the engraftment and function of the HIP p-islet grafts. The immune response against cotransplanted WT and DKO p-islet cells seems targeted and does not appear to affect the survival or endocrine function of HIP p-islet cells. A potential clinical trial with HIP p-islets

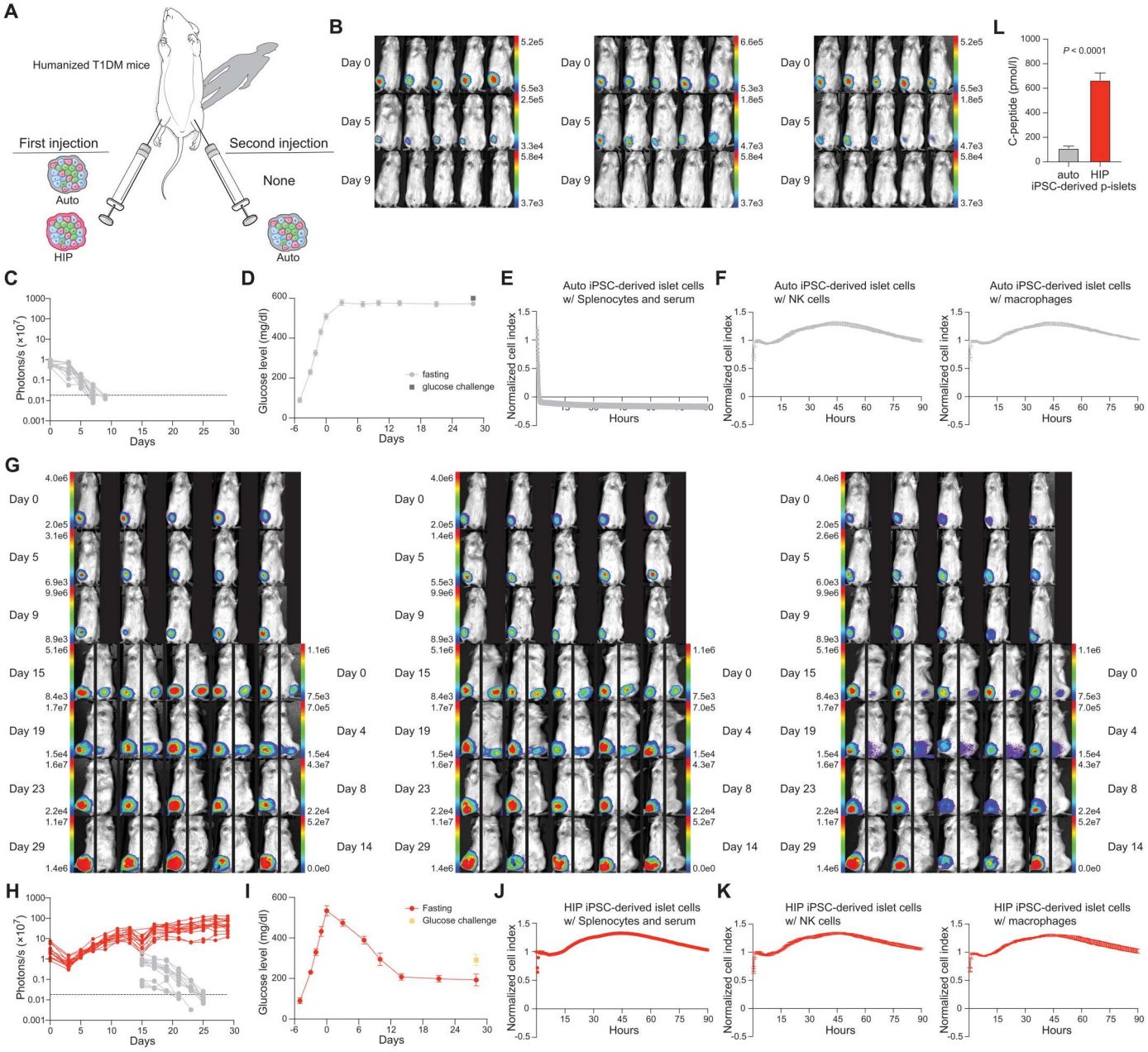

Fig. 6. Human HIP iPSC–derived p-islets survive in an autologous autoimmune diabetes model and alleviate diabetes. (**A**) In one group, auto iPSC–derived p-islets were transplanted in autologous T1DM mice, and survival and glucose were monitored. In another group, HIP iPSC–derived p-islets were transplanted in autologous T1DM mice, followed by subsequent transplantation of auto p-islets on day 15. (**B** and **C**) Three different batches of auto iPSC–derived p-islets were transplanted in autologous T1DM mice. BLI (B) and signals (C) for all 15 animals are shown. (**D**) Fasting blood glucose and 30-min glucose challenge are shown (means ± SD, 15 animals). (**E**) Impedance killing assays with splenocytes and sera from T1DM mice that received auto p-islets were performed against auto p-islet cells (means ± SD, five animals). (**F**) Impedance killing assays were further performed using NK cells or macrophages as effector cells (means ± SD, three independent experiments). (**G** and **H**) Three different batches of HIP iPSC–derived p-islets were transplanted into the right thigh muscles of autologous T1DM mice. BLI (G) and signals (H) for all 15 animals are shown. On day 15, auto iPSC–derived p-islets were transplanted into the left thigh muscle. The BLI scale in (G) on the left side is from the HIP p-islet imaging; the scale on the right is from the auto p-islet imaging. (**I**) Fasting blood glucose and 30-min glucose challenge are shown (means ± SD, 15 animals). (**J**) Impedance killing assays with splenocytes and sera from T1DM mice that received HIP p-islets were performed against HIP p-islet cells (means ± SD, five animals). (**K**) Impedance killing assays were further performed using NK cells or macrophages as effector cells (means ± SD, three independent experiments). (**L**) C-peptide in mice that received auto p-islets or HIP p-islets was measured after 29 days (means ± SD, 15 animals each, two-tailed Student's *t* test).

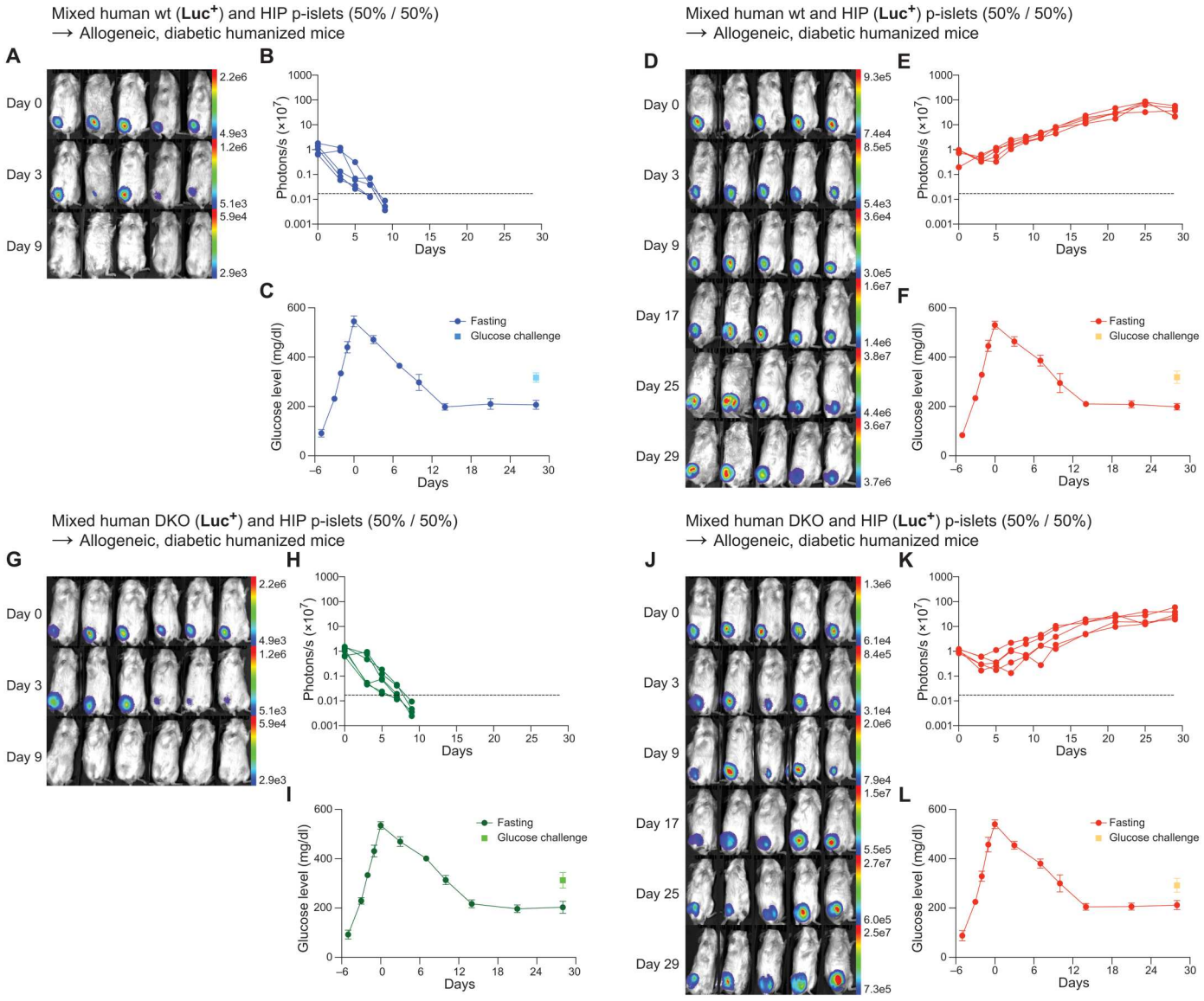

Fig. 7. Human HIP islet cells in mixed p-islets with WT or DKO cells survive in immunocompetent, allogeneic, diabetic humanized mice. (**A** to **F**) Mixed human WT and HIP p-islets were transplanted into allogeneic, diabetic humanized mice. When the WT cells were labeled Luc$^+$, BLI (A) and signals (B) showed a vanishing of this cell population over time (all five animals are shown). In contrast, when the HIP cells were labeled Luc$^+$, BLI (D) and signals (E) showed cell survival (all five animals are shown). In both cases, the transplanted mixed p-islets achieved glycemic control [fasting blood glucose and 30-min glucose challenge are shown; (C and F), five animals per group]. (**G** to **L**) Mixed human DKO and HIP p-islets were transplanted into allogeneic, diabetic humanized mice. When the DKO cells were labeled Luc$^+$, BLI (G) and signals (H) showed a vanishing of this cell population over time (all six animals are shown). In contrast, when the HIP cells were labeled Luc$^+$, BLI (J) and signals (K) showed cell survival (all five animals are shown). In both cases, the transplanted mixed p-islets achieved glycemic control [fasting blood glucose and 30-min glucose challenge are shown; (I), six animals and (L), five animals].

could include initial immunosuppression of the recipients because it is standard for allogeneic islet transplants, with subsequent weaning and discontinuation. To test the susceptibility of our HIP p-islets to immunosuppression-associated β cell toxicity (*33*), we treated allogeneic, diabetic humanized mice with a cocktail of immunosuppressive drugs including tacrolimus, mycophenolate mofetil, and basiliximab. WT (fig. S5, A to C) and HIP (fig. S5, D to F) p-islets showed similar survival, and both alleviated diabetes and showed similar c-peptide concentrations in these immunosuppressed recipients (fig. S5G). Animals in both groups had sufficient tacrolimus trough concentrations of >10 ng/ml (fig. S5H). In the model tested, human HIP p-islets did not appear to require high engineering efficiencies and were not more susceptible to immunosuppression-related toxicity than WT p-islets, both of which features support their advancement toward clinical trials.

Human HIP p-islets can reliably be eliminated by blocking CD47

HIP cells are designed to evade the immune system and thus could also escape immune clearance after undergoing a malignant

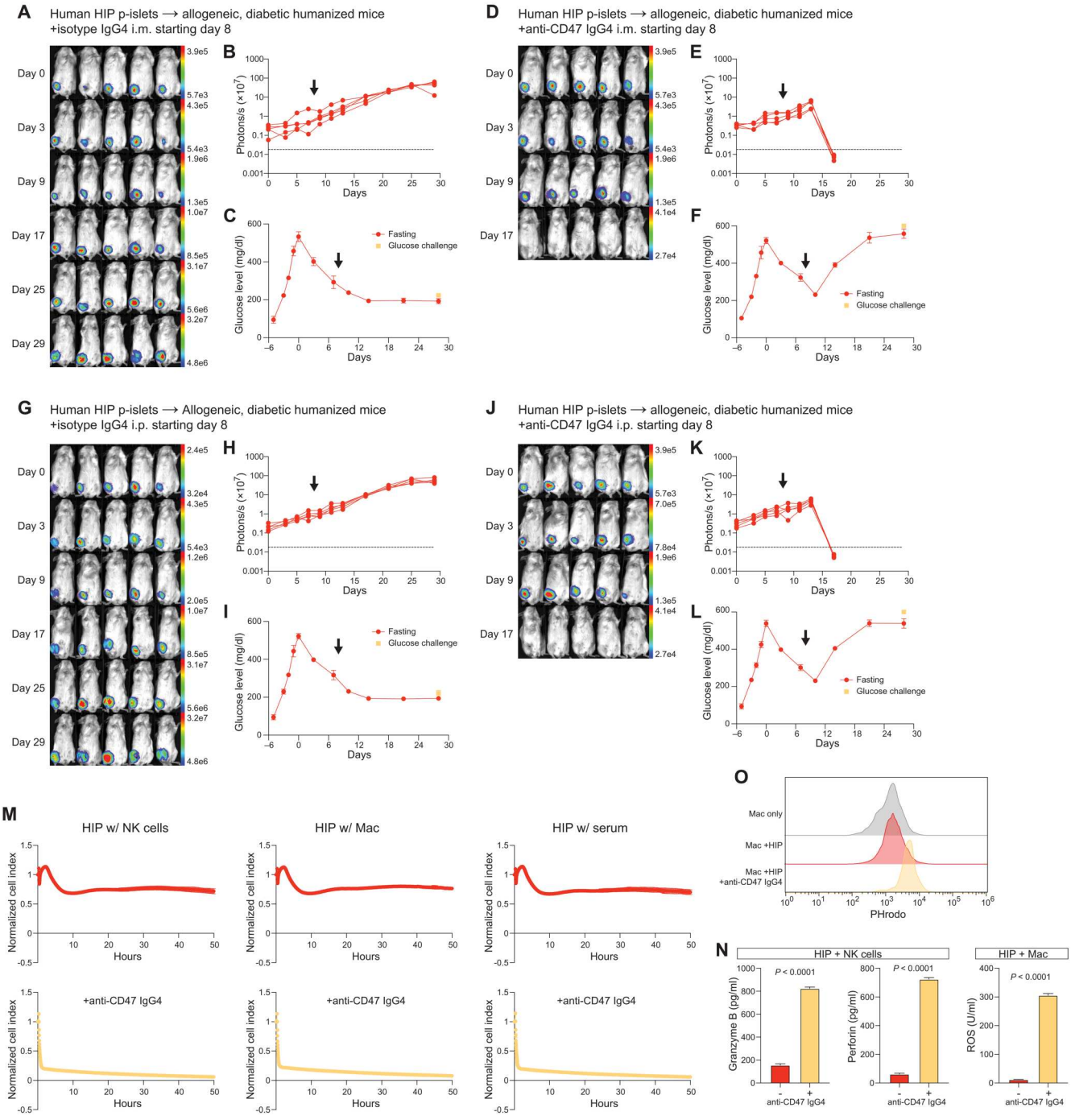

Fig. 8. Human HIP p-islets can reliably be eliminated using a CD47-targeting antibody. (**A** and **B**) Human HIP p-islets were transplanted into allogeneic, diabetic humanized mice. BLI (A) and signals (B) for all five animals are shown. (**C**) Fasting blood glucose and 30-min glucose challenge are shown (means ± SD, five animals). An IgG4 isotype antibody was injected intramuscularly on day 8. (**D** and **E**) Human HIP p-islets were transplanted into allogeneic, diabetic humanized mice. BLI (D) and signals (E) for all five animals are shown. (**F**) Fasting blood glucose and 30-min glucose challenge are shown (means ± SD, five animals). An anti-CD47 IgG4 antibody was injected intramuscularly on day 8. (**G** and **H**) Human HIP p-islets were transplanted into allogeneic, diabetic humanized mice. BLI (G) and signals (H) for all five animals are shown. (**I**) Fasting blood glucose and 30-min glucose challenge are shown (means ± SD, five animals). An IgG4 isotype antibody was injected intraperitoneally on day 8. (**J** and **K**) Human HIP p-islets were transplanted into allogeneic, diabetic humanized mice. BLI (J) and signals (K) for all five animals are shown. (**L**) Fasting blood glucose and 30-min glucose challenge are shown (means ± SD, five animals). An anti-CD47 IgG4 antibody was injected intraperitoneally on day 8. (**M**) Human HIP islet cells were challenged with allogeneic NK cells or macrophages (Mac) in impedance killing assays with or without an anti-CD47 IgG4 antibody (means ± SD, three independent replicates per group and time point). (**N**) Human HIP islet cells were incubated with NK cells and granzyme B and perforin or were incubated with macrophages, and ROS was quantified in supernatant (means ± SD, three independent replicates per group and time point, two-tailed Student's *t* test). (**O**) Human HIP islet cells were incubated with macrophages with or without an anti-CD47 IgG4 antibody, and phagocytosis was measured (one representative image of two independent experiments).

transformation. Although, at this point, this is a theoretical safety risk, we aimed to test a reliable safety strategy to remove all HIP cells when necessary. HIP cells distinguish themselves by their high CD47 surface expression, which we have shown earlier is necessary to avoid innate immune killing. We thus used an anti-CD47 IgG4 antibody currently cleared for clinical trial use. Human HIP p-islets were transplanted into allogeneic, diabetic humanized mice, and, after 8 days, an IgG4 isotope control antibody or the clinical anti-CD47 antibody was administered by intramuscular injection. The isotype antibody had no effect on HIP p-islet survival or endocrine function (Fig. 8, A to C). A few days after the anti-CD47 antibody was given, however, we observed a sharp drop of the BLI signal to below the detection level (Fig. 8, D and E). Fasting blood glucose concentrations, which were downtrending and had almost reached the threshold of 200 mg/dl started to rebound, and all animals became diabetic again (Fig. 8F). When the same experiment was repeated, but with the antibodies given intraperitoneally, we observed the same result, with an effective elimination of the HIP cells by BLI signal and their vanishing endocrine function (Fig. 8, G and L). We also performed additional in vitro testing of the anti-CD47 antibody. Impedance-based killing assays with HIP islet target cells showed that the anti-CD47 IgG4 was capable of mediating cytotoxicity through NK cells and macrophages (Fig. 8M). The anti-CD47 IgG4 triggered granzyme and perforin release by NK cells and reactive oxygen species (ROS) by macrophages, which were additionally triggered to phagocytose the HIP targets (Fig. 8, N and O). These results point to the ability of the anti-CD47 IgG4 antibody to lead to the clearance of HIP cells, its appropriate tissue distribution allowing different administration routes, and its multiple effector mechanisms.

DISCUSSION

We have developed a gene engineering protocol for primary human donor islets that achieves high yield, including high gene editing efficiencies, with minimal cell loss during the engineering process. This enabled us to reliably generate human HIP p-islets with the HLA class I– and class II–deficient and high $CD47^+$ phenotype from several different organ donors. β cells are sensitive to hypoxia and stress during pancreas retrieval and preservation, islet isolation, and culture (*34*). Despite comprising only 1 to 2% of the total pancreatic mass, islets physiologically receive 10 to 20% of the pancreatic blood flow (*35*). Gene editing of primary human islets has been viewed as challenging, and a method with sufficient efficiency has only recently been developed (*36*). Their stepwise protocol included islet dispersion, single gRNA (sgRNA) and Cas9 delivery, and reaggregation of islet cell clusters into p-islets. Dispersed islet cells naturally gravitate toward reaggregation. It has recently been shown that the morphology, size, insulin and glucagon content, and endocrine cell composition of such p-islets remained unchanged compared to that in cultured native islets from the same donor (*37*). We have refined this protocol and have successfully generated HIP p-islets from multiple different human islet donors.

Difficulties with gene editing of primary human islet cells had prompted cotransplantation strategies where an easier-to-edit accompanying cell type was hoped to provide local immune protection. The survival of allogeneic mouse islets could be prolonged, but rejection could not be prevented by cotransplantation of programmed death–ligand 1/cytotoxic T-lymphocyte–associated protein 4 (PD-L1/CTLA4)–Ig–overexpressing mesenchymal stromal cells (*38*) or regulatory T cells (*39*) to foster local immune tolerance. Similarly, cotransplantation of FS-7–associated surface antigen ligand (FasL)–overexpressing myoblasts (*40*) or indoleamine 2,3 dioxygenase–overexpressing fibroblasts (*41*) achieved some improved survival of allogeneic mouse islet grafts. In diabetic nonhuman primates, cotransplantation of allogeneic islets and streptavidin-FasL–presenting microgels under temporary, 3-month high-dose rapamycin immunosuppression achieved a reduction of external insulin requirement and prolonged graft survival (*42*).

Our HIP p-islets completely evaded both allorejection and autoimmunity in immunocompetent, diabetic humanized mouse models and consistently achieved full glycemic control. HIP p-islets not only showed prolonged survival in noninvasive monitoring over allogeneic WT p-islets but also induced no measurable immune response in the recipients. This HIP engineering strategy thus provides immune protection without the need for encapsulation strategies, which have not yet shown therapeutic efficiency (*43*). Alginate microencapsulated islets implanted intraperitoneally in non-immunosuppressed patients with T1DM demonstrated c-peptide secretion for 1 to 2.5 years, but the amount of insulin released was too small to alter blood glucose in a meaningful way (*44*, *45*). Macroencapsulated islets within the bioartificial pancreas βAir, a cell chamber connected to a refillable oxygen tank, survived for 3 to 6 months, but insulin release was minuscule and had no impact on metabolic control (*46*). In the models tested, our HIP p-islets were protected from the immune system and could engraft and be vascularized to best support β cell function.

Pancreatic islets have a dense physiological vascular network with directed blood flow from the core of the islet outward (*47*) and connecting every β cell with a capillary (*48*). We chose an intramuscular implant site because preclinical data showed that the striated muscle established a similar vascular network and showed superiority over intraportally transplanted islets that had few intra-islet vessels (*49*, *50*). The comprehensive revascularization of transplanted islets in our study with gradual improvement of perfusion is reflected by increasing BLI signals during the 28-day observation periods. Clinical islet transplantation into the forearm allows easy access to the grafts (*51*), permits magnetic resonance imaging (*52*) or positron emission tomography (*53*) to follow graft survival, and could be a preferred implant site for clinical use. A single-center, open-label, nonrandomized safety and efficacy trial with patients with T1DM is currently using this intramuscular implant site for the transplantation of allogeneic pancreatic islets (NCT03977662). We are awaiting results because they can inform the design of subsequent studies with HIP p-islets.

Limitations of this study include the shortcomings of animal models for human T1DM, which is a chronic disease with long-term complications that are not reflected in short-duration animal experiments. In addition, whether subtle immune activation can occur in long-term surviving HIP p-islets through indirect presentation remains to be seen. Long-duration studies of HIP p-islet transplants in nonhuman primates may best assess chronic rejection. Furthermore, the longevity of p-islet vitality in the absence of immune rejection remains unclear. Transplanted islets are susceptible to incur loss under conditions of hyperglycemia and stress even in the absence of immune rejection in patients after

autologous islet transplantation (*54*). Patients are advised to frequently monitor their blood glucose three or four times per day with illness, surgery, or severe physical stress. HIP p-islet grafts might therefore still undergo chronic attrition despite complete immune evasiveness.

The generation of pluripotent stem cell–derived islet cells has been developed over the past decade (*55*–*57*), and the transplantation of in vitro-generated, allogeneic islet organoids could become another strategy to treat T1DM not limited by donor scarcity (*58*). The first evidence of meal-regulated insulin secretion by stem cell–derived pancreatic endoderm cells has recently been reported (*59*). Patients in these studies have received non-immunoprotective macroencapsulation devices and were required to be on an immunosuppressive regimen. The main difficulty with this stem cell–based approach has been the generation of functional islet cells releasing insulin in a physiologically regulated fashion (*60*). Although differentiation protocols have been optimized, such in vitro generated islet organoids are currently still less effective than primary donor islets (*61*). The stem cell–based approach, however, is suitable for gene engineering of the starter cell line. Efforts are underway to show proof of concept for HIP iPSC–derived islet cell grafts. However, until the hurdles associated with these cells are fully overcome, HIP-engineered p-islets could become a more near-term solution for many patients with IAH and severe hypoglycemic events to achieve insulin independence.

MATERIALS AND METHODS

Study design

The overall objective of the study was to assess the feasibility of engineered human HIP primary pancreatic islets to fully escape immune rejection in allogeneic recipients and to alleviate diabetes. We first aimed to establish a multistep gene engineering process that allows the editing of human donor islets at high yield despite the fact that islets are organoids known to be sensitive to ischemia and difficult to edit. Human donor islets were purchased from Prodo. To assess allorejection of HIP p-islets using in vivo models, we mainly used humanized mice. All humanized mice included here showed >40% of human $CD45^+$ cells in their peripheral blood and human $CD3^+$ cells >2% of human $CD45^+$ cells. That was to ensure immune competence. To induce diabetes in humanized mice, we injected STZ intraperitoneally. To assess autoimmunity, we used the established NOD mouse model with edited primary allogeneic and syngeneic HIP islet grafts. All NOD mice had established diabetes with glucose >300 mg/dl at the time of inclusion in the study. We then aimed to develop a humanized mouse model for autoimmunity to test our human HIP p-islets. No established model was available at the time. The sample size for the in vivo studies to achieve statistical significance was not calculated before the studies because the survival of the HIP-edited cells in the different mice models was previously unknown. It was reasoned that 3 to 15 mice per group in individual experiments would indicate valid efficacy. All samples were number-coded until the readout was finalized. Animals were number-coded and assigned to a group before cell transplantation. Group allocation for cell transplantations was performed by blinded investigators. For in vivo imaging, the investigators doing the readouts were not blinded but not familiar with the experimental setup of this study. Data that passed the Shapiro-Wilk test for normal distribution were analyzed with parametric tests; otherwise, nonparametric tests were used.

Primary human islets

Gene editing of human primary islets

Human primary cadaveric islets were purchased from Prodo Labs and cultured overnight in PIM media (Prodo). The CRIPSR-Cas9 technology was used for the disruption of the *B2M* and *CIITA* genes. Islet clusters were dissociated in single cells using ACCUMAX (STEMCELL Technologies) for 10 min at 37°C. The gRNA sequences 5′-CGTGAGTAAACCTGAATCTT-3′ and 5′-GATATTGGCATAAGCCTCCC-3′ were used for the human *B2M* gene and human *CIITA* gene, respectively. The Lonza P3 Primary Cell 4D-Nucleofector X Kit (V4XP-3032, Lonza) was used for the transfection of the islet cells. Briefly, cells were transduced with a final concentration of 50 million per ml in P3 buffer. Twenty microliters of the cell suspension were pipetted in one well of the 8-strip containing 13 μg of Cas9 enzyme and 6.5 μg of sgRNA, respectively. Lonza's 4D-Nucleofector was used for the electroporation with the preset program CA-137. Islet cells were transferred into U-bottom 96-well plates containing 50,000 cells per well in PIM(S) media (Prodo) and rested for 1 hour at 37°C and 5% CO_2 before moving the plate on the Belly Dancer orbital shaker (IBI Scientific) for islet reclustering. Complete medium change was performed after 48 hours, and islet clusters were incubated on the Belly Dancer for another 24 hours.

Islet clusters were dissociated again in single cells using ACCUMAX for cell sorting using the anti–HLA-A,B,C antibody (clone G46_2.6, BD Biosciences) or IgG1 isotype–matched control antibody (clone MOPC-21, BD Biosciences) and anti–HLA-DR,DP,DQ antibody (clone Tu3a, BD Biosciences) or IgG2a isotype–matched control antibody (clone G155-178, BD Biosciences). Double-negative cells were sorted in the BD FACSAria II and replated in U-bottom 96-well plates as described above for islet reclustering on the Belly Dancer orbital shaker. After 24 hours, islets were dissociated in single cells for CD47 and luciferase transduction with a CAG-CD47 LVV (custom order, Thermo Fisher Scientific) at a multiplicity of infection (MOI) of 5 and a CAG-luciferase LVV (custom order, GenTarget) at an MOI of 20. Spinfection was performed with the presence of protamine sulfate (10 μg/ml; Fresenius Kabi) at 300*g* for 15 min. Cells were replated in U-bottom 96-well plates as described above for islet reclustering on the Belly Dancer orbital shaker. After 48 hours, cells were dissociated in single cells using ACCUMAX and underwent cell sorting for human CD47 with anti-CD47 antibody (clone B6H12, BD Biosciences) or IgG1 isotype–matched control antibody (clone MOPC-21, BD Biosciences) on a BD FACSAria II. Luciferase expression was confirmed by adding D-luciferin (Promega). Signals were quantified with Ami HT (Spectral Imaging) in maximum photons s^{-1} cm^{-2} sr^{-1}. Islet cells were replated in U-bottom 96-well plates as described above for islet reclustering on the Belly Dancer orbital shaker until transplantation.

Mouse models

Male and female NSG mice (005557; 6 to 12 weeks), female humanized NSG-SGM3 mice (013062; 12 to 18 weeks), female NODShilt/J mice (001976; 6 to 18 weeks), and female C57BL/6J mice (000664) were purchased from the Jackson Laboratory. Male NOD SCID mice (394; 6 to 12 weeks) were purchased from Charles River Laboratories. Humanized mice had to show >40% of human $CD45^+$

cells in their peripheral blood and >2% human $CD3^+$ cells of $hCD45^+$ cells to be included in this study. Female NOD mice developed diabetes at about 12 weeks of age, and only diabetic animals with glucose >300 mg/dl were included. Animals were randomly assigned to experimental groups. Animal experiments were approved by the Explora BioLabs Institutional Animal Care and Use Committee. Animals received humane care, and all experiments followed local guidelines. Mice were housed in 12-hour light/12-hour dark cycles with humidity between 30 and 70% at ambient temperatures of 20° to 26°C. The animal facility is a specific pathogen–free facility. To induce diabetes, mice were injected with STZ intraperitoneally (60 mg/kg; Sigma-Aldrich) for five consecutive days. Islet clusters were injected intramuscularly into the hindlimb muscle with a 27-gauge needle on day 0. Some groups received the anti-CD47 IgG4 antibody magrolimab or the isotype control antibody (both customized; Creative Biolabs) at a dose of 250 μg starting on day 8. The antibody was injected intramuscularly or intraperitoneally. Mice in some groups received immunosuppression. These mice had daily injections of mycophenolate mofetil (MilliporeSigma) at 64 mg/kg and tacrolimus (FK-506, MilliporeSigma) at 5 mg/kg, respectively. On days 0 and 4, all mice additionally received basiliximab (Simulect; anti-Human IL-2RA/CD25 antibody; LSBio) at 0.25 mg/kg. The number of animals per experimental group is presented in each figure.

Cell generation for autologous T1DM model

PBMCs and sera from a volunteer with T1DM were provided by Sanguine BioSciences, and iPSCs were generated by R&D Systems. HIP editing of iPSCs was performed as described above. The islet differentiation was performed as previously described (*61*, *62*).

Imaging of WT and HIP iPSC–derived islet cells

About 20 μl of aggregates were collected into a 1.5-ml Eppendorf tube and washed with stain buffer (Dulbecco's phosphate-buffered saline with 0.1% bovine serum albumin and 5 mM EDTA). Aggregates were stained with 5 μl of phycoerythrin (PE) anti-human CD47 (clone CC2C6, BioLegend) and allophycocyanin (APC) anti-human HLA-ABC (clone G46-2.6, BD Bioscience) for 45 min on ice and washed with stain buffer. Cells were fixed with BD Cytofix on ice for 30 min (Fisher Scientific), washed with stain buffer, mounted on slides with ProLong Gold with 4′,6-diamidino-2-phenylindole (DAPI; Fisher Scientific), and allowed to dry overnight. Slides were then imaged on the Leica THUNDER Imaging System.

Generation of humanized diabetic T1DM mice and transplantation of T1DM iPSC–derived islet cells

NSG mice received daily intraperitoneal injections of STZ for five consecutive days at 60 mg/kg of body weight in 0.1 M citrate buffer to induce diabetes. Blood glucose was determined by glucometer (Accu-Chek Advantage, Roche) in 10-μl blood samples collected by tail vein venipuncture after 4 hours of fasting. Animals with a glucose concentration of >400 mg/dl were served as recipients for immune cell transfer and cell implant. For adoptive transfer of T1DM immune cells, animals were injected intravenously with 10 million T1DM PBMCs 3 days before islet transplantation. One thousand islet clusters were resuspended in 60 μl of sterile saline and injected intramuscularly into the hindlimb muscle with a 23-gauge needle. Glucose tolerance testing was performed at study end point (28 days after cell transplantation). Mice were fasted for 4 hours, and a baseline blood glucose concentration was obtained. A glucose bolus of 2 g/kg was injected intraperitoneally, and blood glucose was measured at 30 min after injection. Blood was collected from study animals, and plasma was stored at −80°C for enzyme-linked immunosorbent assay (ELISA) c-peptide (Mercodia) according to the manufacturer's protocol. In vivo BLI of transplanted iPSC–derived WT and HIP islet cells was performed as described in Supplementary Materials and Methods.

Mouse islets

Mouse primary islets were isolated as previously described (*63*) and cultured in RPMI 1640 phenol red–free, 10% FCS hi, 1% penicillin-streptomycin, and 1% GlutaMAX (mouse islet media; all Gibco). The CRIPSR-Cas9 technology was used for the disruption of the *B2m* and *Ciita* genes. Islet clusters were dissociated in single cells using ACCUMAX (STEMCELL Technologies) for 10 min at 37°C. The gRNA sequences 5′-TTCGGCTTCCCATTCTCCGG-3′ and 5′-GGTCCATCTGGTCATAGAGG-3′ were used for the mouse *B2m* gene and the mouse *Ciita* gene, respectively. The Lonza P3 Primary Cell 4D-Nucleofector X Kit (V4XP-3032, Lonza) was used for the transfection of the islet cells. Briefly, cells were transduced with a final concentration of 50 million per ml in P3 buffer. Twenty microliters of the cell suspension were pipetted in one well of the 8-strip containing 13 μg of Cas9 enzyme and 6.5 μg of sgRNA, respectively. Lonza's 4D-Nucleofector was used for the electroporation with the preset program CA-137. Islet cells were transferred in U-bottom 96-well plates containing 50,000 cells per well in mouse islet media and rested for 1 hour at 37°C and 5% CO_2 before moving the plate on the Belly Dancer orbital shaker (IBI Scientific) for islet reclustering. Complete medium change was performed after 48 hours, and islet clusters were incubated on the Belly Dancer for another 24 hours.

Islet clusters were dissociated again in single cells using ACCUMAX for cell sorting using the anti–major histocompatibility complex (MHC) I antibody (clone 28-14-8, Thermo Fisher Scientific) or IgG2a isotype–matched control antibody and anti–MHC-II antibody (clone M5/114.15.2, Thermo Fisher Scientific) or IgG2b isotype–matched control antibody. Double-negative cells were sorted on the BD FACSAria II and replated in U-bottom 96-well plates as described above for islet reclustering on the Belly Dancer orbital shaker. After 24 hours, islets were dissociated in single cells for Cd47 and luciferase transduction with an EF1a-Cd47 LVV (custom order, Thermo Fisher Scientific) at an MOI of 20 and a CAG-luciferase LVV (custom order, GenTarget) at an MOI of 20. Spinfection was performed with the presence of protamine sulfate (10 μg/ml) at 300*g* for 15 min. Cells were replated in U-bottom 96-well plates as described above for islet reclustering on the Belly Dancer orbital shaker. After 48 hours, cells were dissociated in single cells using ACCUMAX and underwent cell sorting for mouse Cd47 with anti-Cd47 antibody (clone miap301, BD Biosciences) or rat IgG2a isotype–matched control antibody on a BD FACSAria II. Luciferase expression was confirmed by adding D-luciferin (Promega). Signals were quantified with Ami HT (Spectral Imaging) in maximum photons s^{-1} cm^{-2} sr^{-1}. Islet cells were replated in U-bottom 96-well plates as described above for islet reclustering on the Belly Dancer orbital shaker until transplantation.

In vivo experiments

NSG mice or NOD mice were transplanted with islet clusters intramuscularly on day 0. Mice were monitored on day 0, day 3, every other day until day 13, and, subsequently, every 4 days until day 29. Some NSG mice received 10 million splenocytes from NOD

mice on day 11 intraperitoneally as adoptive transfer. The number of animals and different study groups are presented in each figure. BLI and glucose monitoring were performed as described in Supplementary Materials and Methods.

Statistical analysis

Statistical analyses were performed using GraphPad Prism 9 software. Data that passed the Shapiro-Wilk test for normal distribution were analyzed with parametric tests. Analyses of differences between two groups were performed using an unpaired two-tailed Student's *t* test. Statistical analyses of three groups were performed using a one-way analysis of variance (ANOVA) followed by Bonferroni post hoc test. Data that did not show normal distribution were analyzed using the Kruskal-Wallis test with Dunn's multiple comparisons test for three groups. *P* values are provided for significant differences. Not significant is abbreviated to N.S.

Supplementary Materials

This PDF file includes:
Materials and Methods
Figs. S1 to S5

Other Supplementary Material for this manuscript includes the following:
Data files S1 and S2
MDAR Reproducibility Checklist

View/request a protocol for this paper from *Bio-protocol*.

REFERENCES AND NOTES

1. E. K. Sims, A. L. J. Carr, R. A. Oram, L. A. DiMeglio, C. Evans-Molina, 100 years of insulin: Celebrating the past, present and future of diabetes therapy. *Nat. Med.* **27**, 1154–1164 (2021).
2. L. A. DiMeglio, C. Evans-Molina, R. A. Oram, Type 1 diabetes. *Lancet* **391**, 2449–2462 (2018).
3. S. J. Livingstone, D. Levin, H. C. Looker, R. S. Lindsay, S. H. Wild, N. Joss, G. Leese, P. Leslie, R. J. McCrimmon, W. Metcalfe, J. A. McKnight, A. D. Morris, D. W. M. Pearson, J. R. Petrie, S. Philip, N. A. Sattar, J. P. Traynor, H. M. Colhoun; Scottish Diabetes Research Network Epidemiology Group; Scottish Renal Registry, Estimated life expectancy in a Scottish cohort with type 1 diabetes, 2008-2010. *JAMA* **313**, 37–44 (2015).
4. Y. K. Lin, S. J. Fisher, R. Pop-Busui, Hypoglycemia unawareness and autonomic dysfunction in diabetes: Lessons learned and roles of diabetes technologies. *J. Diabetes Investig.* **11**, 1388–1402 (2020).
5. W. L. Clarke, D. J. Cox, L. A. Gonder-Frederick, D. Julian, D. Schlundt, W. Polonsky, Reduced awareness of hypoglycemia in adults with IDDM. A prospective study of hypoglycemic frequency and associated symptoms. *Diabetes Care* **18**, 517–522 (1995).
6. UK Hypoglycaemia Study Group, Risk of hypoglycaemia in types 1 and 2 diabetes: Effects of treatment modalities and their duration. *Diabetologia* **50**, 1140–1147 (2007).
7. U. Pedersen-Bjergaard, S. Pramming, S. R. Heller, T. M. Wallace, A. K. Rasmussen, H. V. Jorgensen, D. R. Matthews, P. Hougaard, B. Thorsteinsson, Severe hypoglycaemia in 1076 adult patients with type 1 diabetes: Influence of risk markers and selection. *Diabetes Metab. Res. Rev.* **20**, 479–486 (2004).
8. Juvenile Diabetes Research Foundation Continuous Glucose Monitoring Study Group, W. V. Tamborlane, R. W. Beck, B. W. Bode, B. Buckingham, H. P. Chase, R. Clemons, R. Fiallo-Scharer, L. A. Fox, L. K. Gilliam, I. B. Hirsch, E. S. Huang, C. Kollman, A. J. Kowalski, L. Laffel, J. M. Lawrence, J. Lee, N. Mauras, M. O'Grady, K. J. Ruedy, M. Tansey, E. Tsalikian, S. Weinzimer, D. M. Wilson, H. Wolpert, T. Wysocki, D. Xing, Continuous glucose monitoring and intensive treatment of type 1 diabetes. *N. Engl. J. Med.* **359**, 1464–1476 (2008).
9. K. J. Ruedy, C. G. Parkin, T. D. Riddlesworth, C. Graham; DIAMOND Study Group, Continuous glucose monitoring in older adults with type 1 and type 2 diabetes using multiple daily injections of insulin: Results from the DIAMOND Trial. *J. Diabetes Sci. Technol.* **11**, 1138–1146 (2017).
10. L. M. Laffel, L. G. Kanapka, R. W. Beck, K. Bergamo, M. A. Clements, A. Criego, D. J. DeSalvo, R. Goland, K. Hood, D. Liljenquist, L. H. Messer, R. Monzavi, T. J. Mouse, P. Prahalad, J. Sherr, J. H. Simmons, R. P. Wadwa, R. S. Weinstock, S. M. Willi, K. M. Miller; CGM Intervention in Teens and Young Adults with T1D (CITY) Study Group; CDE10, Effect of continuous glucose monitoring on glycemic control in adolescents and young adults with type 1 diabetes: A randomized clinical trial. *JAMA* **323**, 2388–2396 (2020).
11. E. Bekiari, K. Kitsios, H. Thabit, M. Tauschmann, E. Athanasiadou, T. Karagiannis, A.-B. Haidich, R. Hovorka, A. Tsapas, Artificial pancreas treatment for outpatients with type 1 diabetes: Systematic review and meta-analysis. *BMJ* **361**, k1310 (2018).
12. C. K. Boughton, S. Hartnell, H. Thabit, T. Poettler, D. Herzig, M. E. Wilinska, N. L. Ashcroft, J. Sibayan, N. Cohen, P. Calhoun, L. Bally, J. K. Mader, M. Evans, L. Leelarathna, R. Hovorka, Hybrid closed-loop glucose control with faster insulin aspart compared with standard insulin aspart in adults with type 1 diabetes: A double-blind, multicentre, multinational, randomized, crossover study. *Diabetes Obes. Metab.* **23**, 1389–1396 (2021).
13. K. D. Barnard, T. Wysocki, H. Thabit, M. L. Evans, S. Amiel, S. Heller, A. Young, R. Hovorka, C. Angela, Psychosocial aspects of closed- and open-loop insulin delivery: Closing the loop in adults with type 1 diabetes in the home setting. *Diabet. Med.* **32**, 601–608 (2015).
14. A. M. Brooks, N. Walker, A. Aldibbiat, S. Hughes, G. Jones, J. de Havilland, P. Choudhary, G. C. Huang, N. Parrott, N. W. A. McGowan, J. Casey, L. Mumford, P. Barker, K. Burling, R. Hovorka, M. Walker, R. M. Smith, S. Forbes, M. K. Rutter, S. Amiel, M. J. Rosenthal, P. Johnson, J. A. M. Shaw, Attainment of metabolic goals in the integrated UK islet transplant program with locally isolated and transported preparations. *Am. J. Transplant.* **13**, 3236–3243 (2013).
15. B. J. Hering, W. R. Clarke, N. D. Bridges, T. L. Eggerman, R. Alejandro, M. D. Bellin, K. Chaloner, C. W. Czarniecki, J. S. Goldstein, L. G. Hunsicker, D. B. Kaufman, O. Korsgren, C. P. Larsen, X. Luo, J. F. Markmann, A. Naji, J. Oberholzer, A. M. Posselt, M. R. Rickels, C. Ricordi, M. A. Robien, P. A. Senior, A. M. J. Shapiro, P. G. Stock, N. A. Turgeon; Clinical Islet Transplantation Consortium, Phase 3 trial of transplantation of human islets in type 1 diabetes complicated by severe hypoglycemia. *Diabetes Care* **39**, 1230–1240 (2016).
16. J. F. Markmann, M. R. Rickels, T. L. Eggerman, N. D. Bridges, D. E. Lafontant, J. Qidwai, E. Foster, W. R. Clarke, M. Kamoun, R. Alejandro, M. D. Bellin, K. Chaloner, C. W. Czarniecki, J. S. Goldstein, B. J. Hering, L. G. Hunsicker, D. B. Kaufman, O. Korsgren, C. P. Larsen, X. Luo, A. Naji, J. Oberholzer, A. M. Posselt, C. Ricordi, P. A. Senior, A. M. J. Shapiro, P. G. Stock, N. A. Turgeon, Phase 3 trial of human islet-after-kidney transplantation in type 1 diabetes. *Am. J. Transplant.* **21**, 1477–1492 (2021).
17. J. R. N. Lemos, D. A. Baidal, C. Ricordi, V. Fuenmayor, A. Alvarez, R. Alejandro, Survival after islet transplantation in subjects with type 1 diabetes: Twenty-year follow-up. *Diabetes Care* **44**, e67–e68 (2021).
18. B. A. Marfil-Garza, S. Imes, K. Verhoeff, J. Hefler, A. Lam, K. Dajani, B. Anderson, D. O'Gorman, T. Kin, D. Bigam, P. A. Senior, A. M. J. Shapiro, Pancreatic islet transplantation in type 1 diabetes: 20-year experience from a single-centre cohort in Canada. *Lancet Diabetes Endocrinol.* **10**, 519–532 (2022).
19. P. Witkowski, L. H. Philipson, D. B. Kaufman, L. E. Ratner, M. S. Abouljoud, M. D. Bellin, J. B. Buse, F. Kandeel, P. G. Stock, D. C. Mulligan, J. F. Markmann, T. Kozlowski, K. A. Andreoni, R. Alejandro, D. A. Baidal, M. A. Hardy, A. Wickrema, R. G. Mirmira, J. Fung, Y. T. Becker, M. A. Josephson, P. J. Bachul, J. S. Pyda, M. Charlton, J. M. Millis, J. L. Gaglia, R. J. Stratta, J. A. Fridell, S. V. Niederhaus, R. C. Forbes, K. Jayant, R. P. Robertson, J. S. Odorico, M. F. Levy, R. C. Harland, P. L. Abrams, O. K. Olaitan, R. Kandaswamy, J. R. Wellen, A. J. Japour, C. S. Desai, B. Naziruddin, A. N. Balamurugan, R. N. Barth, C. Ricordi; "Islets for US" Collaborative, The demise of islet allotransplantation in the United States: A call for an urgent regulatory update. *Am. J. Transplant.* **21**, 1365–1375 (2021).
20. B. Naziruddin, S. Iwahashi, M. A. Kanak, M. Takita, T. Itoh, M. F. Levy, Evidence for instant blood-mediated inflammatory reaction in clinical autologous islet transplantation. *Am. J. Transplant.* **14**, 428–437 (2014).
21. M. A. Kanak, M. Takita, F. Kunnathodi, M. C. Lawrence, M. F. Levy, B. Naziruddin, Inflammatory response in islet transplantation. *Int. J. Endocrinol.* **2014**, 451035 (2014).
22. C. Dai, J. T. Walker, A. Shostak, A. Padgett, E. Spears, S. Wisniewski, G. Poffenberger, R. Aramandla, E. D. Dean, N. Prasad, S. E. Levy, D. L. Greiner, L. D. Shultz, R. Bottino, A. C. Powers, Tacrolimus- and sirolimus-induced human β cell dysfunction is reversible and preventable. *JCI Insight* **5**, e130770 (2020).
23. J. H. Kim, Y. H. Lee, B. J. Lim, H. J. Jeong, P. K. Kim, J. I. Shin, Influence of cyclosporine A on glomerular growth and the effect of mizoribine and losartan on cyclosporine nephrotoxicity in young rats. *Sci. Rep.* **6**, 22374 (2016).
24. M. Naesens, D. R. J. Kuypers, M. Sarwal, Calcineurin inhibitor nephrotoxicity. *Clin. J. Am. Soc. Nephrol.* **4**, 481–508 (2009).
25. L. E. Higdon, J. C. Tan, J. S. Maltzman, Infection, rejection, and the connection. *Transplantation* **107**, 584–595 (2023).
26. I. Rama, J. M. Grinyo, Malignancy after renal transplantation: The role of immunosuppression. *Nat. Rev. Nephrol.* **6**, 511–519 (2010).
27. M. Wunderlich, F.-S. Chou, K. A. Link, B. Mizukawa, R. L. Perry, M. Carroll, J. C. Mulloy, AML xenograft efficiency is significantly improved in NOD/SCID-IL2RG mice constitutively expressing human SCF, GM-CSF and IL-3. *Leukemia* **24**, 1785–1788 (2010).

28. E. Yoshihara, C. O'Connor, E. Gasser, Z. Wei, T. G. Oh, T. W. Tseng, D. Wang, F. Cayabyab, Y. Dai, R. T. Yu, C. Liddle, A. R. Atkins, M. Downes, R. M. Evans, Immune-evasive human islet-like organoids ameliorate diabetes. *Nature* **586**, 606–611 (2020).
29. T. Deuse, X. Hu, A. Gravina, D. Wang, G. Tediashvili, C. De, W. O. Thayer, A. Wahl, J. V. Garcia, H. Reichenspurner, M. M. Davis, L. L. Lanier, S. Schrepfer, Hypoimmunogenic derivatives of induced pluripotent stem cells evade immune rejection in fully immunocompetent allogeneic recipients. *Nat. Biotechnol.* **37**, 252–258 (2019).
30. Y.-G. Chen, C. E. Mathews, J. P. Driver, The role of NOD mice in type 1 diabetes research: Lessons from the past and recommendations for the future. *Front. Endocrinol. (Lausanne)* **9**, 51 (2018).
31. E. Melanitou, D. Devendra, E. Liu, D. Miao, G. S. Eisenbarth, Early and quantal (by litter) expression of insulin autoantibodies in the nonobese diabetic mice predict early diabetes onset. *J. Immunol.* **173**, 6603–6610 (2004).
32. S. Gregori, N. Giarratana, S. Smiroldo, L. Adorini, Dynamics of pathogenic and suppressor T cells in autoimmune diabetes development. *J. Immunol.* **171**, 4040–4047 (2003).
33. E. B. Rangel, Tacrolimus in pancreas transplant: A focus on toxicity, diabetogenic effect and drug-drug interactions. *Expert Opin. Drug Metab. Toxicol.* **10**, 1585–1605 (2014).
34. J. R. T. Lakey, P. W. Burridge, A. M. J. Shapiro, Technical aspects of islet preparation and transplantation. *Transpl. Int.* **16**, 613–632 (2003).
35. L. Jansson, P.-O. Carlsson, Pancreatic blood flow with special emphasis on blood perfusion of the Islets of langerhans. *Compr. Physiol.* **9**, 799–837 (2019).
36. R. J. Bevacqua, X. Dai, J. Y. Lam, X. Gu, M. S. H. Friedlander, K. Tellez, I. Miguel-Escalada, S. Bonas-Guarch, G. Atla, W. Zhao, S. H. Kim, A. A. Dominguez, L. S. Qi, J. Ferrer, P. E. MacDonald, S. K. Kim, CRISPR-based genome editing in primary human pancreatic islet cells. *Nat. Commun.* **12**, 2397 (2021).
37. J. T. Walker, R. Haliyur, H. A. Nelson, M. Ishahak, G. Poffenberger, R. Aramandla, C. Reihsmann, J. R. Luchsinger, D. C. Saunders, P. Wang, A. Garcia-Ocana, R. Bottino, A. Agarwal, A. C. Powers, M. Brissova, Integrated human pseudoislet system and microfluidic platform demonstrate differences in GPCR signaling in islet cells. *JCI Insight* **5**, e137017 (2020).
38. X. Wang, K. Wang, M. Yu, D. Velluto, X. Hong, B. Wang, A. Chiu, J. M. Melero-Martin, A. A. Tomei, M. Ma, Engineered immunomodulatory accessory cells improve experimental allogeneic islet transplantation without immunosuppression. *Sci. Adv.* **8**, eabn0071 (2022).
39. N. Takemoto, S. Konagaya, R. Kuwabara, H. Iwata, Coaggregates of regulatory T cells and islet cells allow long-term graft survival in liver without immunosuppression. *Transplantation* **99**, 942–947 (2015).
40. H. T. Lau, M. Yu, A. Fontana, C. J. Stoeckert Jr., Prevention of islet allograft rejection with engineered myoblasts expressing FasL in mice. *Science* **273**, 109–112 (1996).
41. R. B. Jalili, F. Forouzandeh, A. M. Rezakhanlou, R. Hartwell, A. Medina, G. L. Warnock, B. Larijani, A. Ghahary, Local expression of indoleamine 2,3 dioxygenase in syngeneic fibroblasts significantly prolongs survival of an engineered three-dimensional islet allograft. *Diabetes* **59**, 2219–2227 (2010).
42. J. Lei, M. M. Coronel, E. S. Yolcu, H. Deng, O. Grimany-Nuno, M. D. Hunckler, V. Ulker, Z. Yang, K. M. Lee, A. Zhang, H. Luo, C. W. Peters, Z. Zou, T. Chen, Z. Wang, C. S. McCoy, I. A. Rosales, J. F. Markmann, H. Shirwan, A. J. Garcia, FasL microgels induce immune acceptance of islet allografts in nonhuman primates. *Sci. Adv.* **8**, eabm9881 (2022).
43. H. P. Dang, H. Chen, T. R. Dargaville, B. E. Tuch, Cell delivery systems: Toward the next generation of cell therapies for type 1 diabetes. *J. Cell. Mol. Med.* **26**, 4756–4767 (2022).
44. R. Calafiore, G. Basta, G. Luca, A. Lemmi, M. P. Montanucci, G. Calabrese, L. Racanicchi, F. Mancuso, P. Brunetti, Microencapsulated pancreatic islet allografts into nonimmunosuppressed patients with type 1 diabetes: First two cases. *Diabetes Care* **29**, 137–138 (2006).
45. B. E. Tuch, G. W. Keogh, L. J. Williams, W. Wu, J. L. Foster, V. Vaithilingam, R. Philips, Safety and viability of microencapsulated human islets transplanted into diabetic humans. *Diabetes Care* **32**, 1887–1889 (2009).
46. P.-O. Carlsson, D. Espes, A. Sedigh, A. Rotem, B. Zimerman, H. Grinberg, T. Goldman, U. Barkai, Y. Avni, G. T. Westermark, L. Carlbom, H. Ahlstrom, O. Eriksson, J. Olerud, O. Korsgren, Transplantation of macroencapsulated human islets within the bioartificial pancreas βAir to patients with type 1 diabetes mellitus. *Am. J. Transplant.* **18**, 1735–1744 (2018).
47. L. R. Nyman, K. S. Wells, W. S. Head, M. McCaughey, E. Ford, M. Brissova, D. W. Piston, A. C. Powers, Real-time, multidimensional in vivo imaging used to investigate blood flow in mouse pancreatic islets. *J. Clin. Invest.* **118**, 3790–3797 (2008).
48. S. Bonner-Weir, Morphological evidence for pancreatic polarity of beta-cell within islets of Langerhans. *Diabetes* **37**, 616–621 (1988).
49. G. Christoffersson, J. Henriksnas, L. Johansson, C. Rolny, H. Ahlstrom, J. Caballero-Corbalan, R. Segersvard, J. Permert, O. Korsgren, P.-O. Carlsson, M. Phillipson, Clinical and experimental pancreatic islet transplantation to striated muscle: Establishment of a vascular system similar to that in native islets. *Diabetes* **59**, 2569–2578 (2010).
50. J. Svensson, J. Lau, M. Sandberg, P.-O. Carlsson, High vascular density and oxygenation of pancreatic islets transplanted in clusters into striated muscle. *Cell Transplant.* **20**, 783–788 (2011).
51. F. Pattou, J. Kerr-Conte, D. Wild, GLP-1-receptor scanning for imaging of human beta cells transplanted in muscle. *N. Engl. J. Med.* **363**, 1289–1290 (2010).
52. C. Toso, J.-P. Vallee, P. Morel, F. Ris, S. Demuylder-Mischler, M. Lepetit-Coiffe, N. Marangon, F. Saudek, A. M. James Shapiro, D. Bosco, T. Berney, Clinical magnetic resonance imaging of pancreatic islet grafts after iron nanoparticle labeling. *Am. J. Transplant.* **8**, 701–706 (2008).
53. O. Eriksson, T. Eich, A. Sundin, A. Tibell, G. Tufveson, H. Andersson, M. Felldin, A. Foss, L. Kyllonen, B. Langstrom, B. Nilsson, O. Korsgren, T. Lundgren, Positron emission tomography in clinical islet transplantation. *Am. J. Transplant.* **9**, 2816–2824 (2009).
54. M. D. Bellin, S. J. Schwarzenberg, M. Cook, D. E. R. Sutherland, S. Chinnakotla, Pediatric autologous islet transplantation. *Curr. Diab. Rep.* **15**, 67 (2015).
55. E. Kroon, L. A. Martinson, K. Kadoya, A. G. Bang, O. G. Kelly, S. Eliazer, H. Young, M. Richardson, N. G. Smart, J. Cunningham, A. D. Agulnick, K. A. D'Amour, M. K. Carpenter, E. E. Baetge, Pancreatic endoderm derived from human embryonic stem cells generates glucose-responsive insulin-secreting cells in vivo. *Nat. Biotechnol.* **26**, 443–452 (2008).
56. A. Rezania, J. E. Bruin, P. Arora, A. Rubin, I. Batushansky, A. Asadi, S. O'Dwyer, N. Quiskamp, M. Mojibian, T. Albrecht, Y. H. C. Yang, J. D. Johnson, T. J. Kieffer, Reversal of diabetes with insulin-producing cells derived in vitro from human pluripotent stem cells. *Nat. Biotechnol.* **32**, 1121–1133 (2014).
57. F. W. Pagliuca, J. R. Millman, M. Gurtler, M. Segel, A. Van Dervort, J. H. Ryu, Q. P. Peterson, D. Greiner, D. A. Melton, Generation of functional human pancreatic β cells in vitro. *Cell* **159**, 428–439 (2014).
58. J. B. Sneddon, Q. Tang, P. Stock, J. A. Bluestone, S. Roy, T. Desai, M. Hebrok, Stem cell therapies for treating diabetes: Progress and remaining challenges. *Cell Stem Cell* **22**, 810–823 (2018).
59. A. Ramzy, D. M. Thompson, K. A. Ward-Hartstonge, S. Ivison, L. Cook, R. V. Garcia, J. Loyal, P. T. W. Kim, G. L. Warnock, M. K. Levings, T. J. Kieffer, Implanted pluripotent stem-cell-derived pancreatic endoderm cells secrete glucose-responsive C-peptide in patients with type 1 diabetes. *Cell Stem Cell* **28**, 2047–2061.e5 (2021).
60. A. M. J. Shapiro, D. Thompson, T. W. Donner, M. D. Bellin, W. Hsueh, J. Pettus, J. Wilensky, M. Daniels, R. M. Wang, E. P. Brandon, M. S. Jaiman, E. J. Kroon, K. A. D'Amour, H. L. Foyt, Insulin expression and C-peptide in type 1 diabetes subjects implanted with stem cell-derived pancreatic endoderm cells in an encapsulation device. *Cell Rep. Med.* **2**, 100466 (2021).
61. N. J. Hogrebe, K. G. Maxwell, P. Augsornworawat, J. R. Millman, Generation of insulin-producing pancreatic β cells from multiple human stem cell lines. *Nat. Protoc.* **16**, 4109–4143 (2021).
62. J. R. Millman, C. Xie, A. Van Dervort, M. Gurtler, F. W. Pagliuca, D. A. Melton, Generation of stem cell-derived β-cells from patients with type 1 diabetes. *Nat. Commun.* **7**, 11463 (2016).
63. D.-S. Li, Y.-H. Yuan, H.-J. Tu, Q.-L. Liang, L.-J. Dai, A protocol for islet isolation from mouse pancreas. *Nat. Protoc.* **4**, 1649–1652 (2009).

Acknowledgments: We thank M. Nguyen-McCarty, A. Gagnon, and D. Galvez for characterization of stage 6 differentiated islet cells and R. De Jesus for providing HIP editing reagents. We also thank A. Dominguez for contribution in supporting the HIP edit work of the T1DM iPSCs and V. Nguyen for mouse islet isolation and overall assistance with cell sorting experiments. We thank K. Copeland and B. Nelson (Spectral Instruments Inc.) for technical support. Medical illustration was done by J. A. Klein of Mito Pop. **Funding:** All studies were funded by Sana Biotechnology Inc. **Author contributions:** X.H. performed all immunobiology experiments, molecular biology, islet and glucose studies, islet cell culture, and editing work and analyzed the data. C.G. performed and analyzed all BLI experiments using human cells. A.M.F. lead the cell sourcing and generation of iPSCs, and K.W. performed in vivo injections and mouse islet cell BLI. C.Y. performed the in vitro immunofluorescence staining and imaging. R.B. performed BLI. M.L. analyzed xCELLigence and, together with C.Y., F.W., and A.G.O., processed in vivo tissue and generated cell suspensions. A.G.O. and A.J.C. performed in vivo histopathology and analyzed the data. R.A. and W.E.D. generated the HIP edits in iPSCs. A.L., K.E., J.M.R., and J.R.M. generated iPSC-derived T1DM islet cells. T.D. evaluated the data, developed and produced the figures, and co-wrote the manuscript with S.S. S.S. conceptualized and designed the experiments, supervised the project, and co-wrote the manuscript with T.D. All authors helped edit the manuscript. **Competing interests:** All experiments were conducted by or on behalf of Sana Biotechnology Inc., and no data from UCSF or Washington University in St. Louis were used. A.J.C. and T.D. performed the work in this manuscript as consultants to Sana Biotechnology Inc. T.D. owns stock in Sana Biotechnology Inc. J.R.M. is employed by Washington University in St. Louis. All other authors are employees of and own stock in Sana Biotechnology Inc. X.H. and S.S. are inventors on a patent (International Application No: PCT/US2022/074878; title "Genetically modified primary cells for allogeneic cell therapy"). **Data and materials availability:** All data associated with this study are present in the paper or the

Supplementary Materials. Raw data from figures are in data file S1, and antibodies used are in data file S2. Correspondence and requests for materials should be addressed to S.S (sonja.schrepfer@sana.com). The following materials are restricted: gene editing reagents (supplier's label license prohibits transfer to third party), primary islet cells (human and mouse: cells are only viable in culture short term and cannot be frozen). Pluripotent stem cells are available under a material transfer agreement with FUJIFILM Cellular Dynamics Inc..

Submitted 7 January 2023
Accepted 23 March 2023
Published 12 April 2023
10.1126/scitranslmed.adg5794

Science Translational Medicine

Human hypoimmune primary pancreatic islets avoid rejection and autoimmunity and alleviate diabetes in allogeneic humanized mice

Xiaomeng Hu, Corie Gattis, Ari G. Olroyd, Annabelle M. Friera, Kathy White, Chi Young, Ron Basco, Meghan Lamba, Frank Wells, Ramya Ankala, William E. Dowdle, August Lin, Kyla Egenberger, J. Michael Rukstalis, Jeffrey R. Millman, Andrew J. Connolly, Tobias Deuse, and Sonja Schrepfer

Sci. Transl. Med., **15** (691), eadg5794.
DOI: 10.1126/scitranslmed.adg5794